Modeling and Control of the Open Plate Reactor

Haugwitz, Staffan

2005

Document Version:
Publisher's PDF, also known as Version of record

Modeling and Control of the Open Plate Reactor

Staffan Haugwitz

Department of Automatic Control
Lund Institute of Technology
Lund, September 2005

Department of Automatic Control
Lund Institute of Technology
Box 118
SE-221 00 LUND
Sweden

ISSN 0280–5316
ISRN LUTFD2/TFRT--3237--SE

Printed in Sweden,
Lund University, Lund 2005

Abstract

The focus of this thesis is on modeling and control of the Open Plate Reactor (OPR), a new heat exchange reactor being developed by Alfa Laval AB. It combines intensified mixing with enhanced heat transfer capacity into one operation. With the novel concept, highly exothermic reactions can be produced using more concentrated reactants, thus saving time and energy in the subsequent separation stage. To better utilize the reactor, reactants can be injected in multiple injection points and there are internal sensors for process monitoring and control. A flexible process configuration simplifies the adaptation of the reactor to new reactions in terms of residence time, cooling system, actuator and sensor locations. To take full advantage of the flexible configuration and the improved performance, a new process control system is presented.

A nonlinear model of the reactor is derived from first principles. After steady-state and dynamic analyses of the OPR, suitable control variables are chosen to allow flexible and accurate control of the reactor temperature and concentration. A Model Predictive Controller (MPC) is designed to maximize the conversion under hard input and temperature constraints. An extended Kalman filter estimates unmeasured concentrations and parameters, to increase the robustness to process variations. The MPC sends reference signals to local feedback controllers within a cascade control structure. To remove the generated heat from the reaction, a cooling system is designed and experimentally verified. For temperature control, a mid-ranging control technique is implemented to increase the operating range of the hydraulic equipment and to increase the robustness to disturbances. Dynamic simulation and optimization show that the designed control system leads to high conversion and ensures that the temperature inside the reactor does not exceed a pre-defined safety limit.

Acknowledgment

Already the very first month of my PhD studies, I participated in a CPDC course in patent rights. The two-day course was concluded with a visit to Alfa Laval in Lund. There Tommy Norén introduced us to this new concept of Open Plate Reactors. Even though he shouldn't say too much, due to the patents being filed at the time, he was incredibly enthusiastic about this project and couldn't stop himself from preaching about its promising potentials. And from that moment I have had the pleasure to work on this project, Advanced Reactor Technology (ART).

Joining this international project, ART, as a fresh PhD student was very interesting and challenging. My supervisor Per Hagander has been my main support and we have had many long rewarding discussions about the project and research in general. I am very grateful for all the time he has given me. He has very elegantly guided me from the initial months as a newbie up till now, giving me more and more freedom and responsibility along the way. Tore Hägglund has also been valuable as co-supervisor.

My time at the department have indeed been a joyful time, which you all probably can see on my big smile. I am very fond of the trinity of the PhD program; the research, the courses and the teaching, which constitutes a well-balanced mixture. However, it is the people at the department that elevates this job from good to great, with the coffee breaks, Christmas parties, Ultimate Frisbee sessions, floor hockey and last but not least, all the rewarding discussions with my colleagues, whom I can go to with any questions. My roommate Tomas Olsson deserves a special thanks for the patience when answering all my questions on control and non-control topics. Another significant person is Anders Robertsson, who always has time for everyone and an interest to help. Johan Åkesson has been a mentor for me and his MPC knowledge and algorithms were essential for the award-winning article at IFAC in Prague, for which he deserves a credit. I have also enjoyed the numerous hikes and board game sessions with Johan Bengtsson.

Within the ART project I had the pleasure of working with experts from many different fields outside the control area, whom I all would like to thank. The discussions have been rewarding and given me an extensive view of chemical processes, heat transfer and reaction kinetics as well as splendid dinners and project meetings. In particular

I would like to acknowledge Tommy Norén, Barry Johnson, Fabrice Chopard, Sébastien Elgue and Kasper Höglund from Alfa Laval.

One part of the project included experiments on the process in the laboratory at Alfa Laval in Lund. There I appreciated the help of Bengt Göland and Michel Granath.

My very first few steps towards a PhD career was taken at University of California in Santa Barbara (UCSB), where I took graduate classes in control engineering during my undergraduate exchange year. It would not have been possible without the influential help from Karl Johan Åström and Petar Kokotovic to overcome the bureaucratic obstacles. I also want to thank Anders Åberg, who inspired and supported me to pursue a PhD, while supervising my master's thesis.

Finally I would like to thank my non-controlled friends and family, for all the fun we have in terms of sailing, skiing, hikes and parties.

This project has been funded by the Centre of Process Control and Design, CPDC, the Swedish Foundation for Strategic Research, SSF and by Alfa Laval AB. The workshops and meetings of CPDC has been interesting and special thanks goes to Bernt Nilsson, the coordinator of CPDC. For the experimental part, there was a generous equipment grant from National Instruments.

Contents

1

Introduction

1.1 Background and motivation

The syntheses of fine chemicals or pharmaceuticals, widely carried out in batch or semi-batch reactors, are often strongly limited by constraints related to the dissipation of the heat generated by the reactions. A common solution is to dilute the chemicals to lower concentrations, thus ensuring that the reaction rate and therefore also the heat release is lower than the heat transfer capacity of the reactor. After the reaction stage, the solvent is removed in a separation stage to provide a high-concentrated product with good quality. This separation process is both time and energy consuming, thus very expensive.

To reduce these problems, the Advanced Reactor Technology (ART) project was initiated by Alfa Laval AB in 2002. Its objective is to design new types of reactors through process intensification (PI), where new methods and equipment are developed with the goal of allowing cleaner and more energy-efficient production in smaller reactors. The reduction in size also leads to increased safety with smaller amounts of hazardous chemicals being in use at each time. The field of PI has been an active research area since the 1980's, see for example [Ramshaw, 1995], [Green *et al.*, 1999] and [Stankiewicz and Moulin, 2000]. One example of PI innovation is the compact heat exchangers, which has been widely successful in many applications. However, attempts to use heat exchangers as chemical reactors, to utilize their high heat trans-

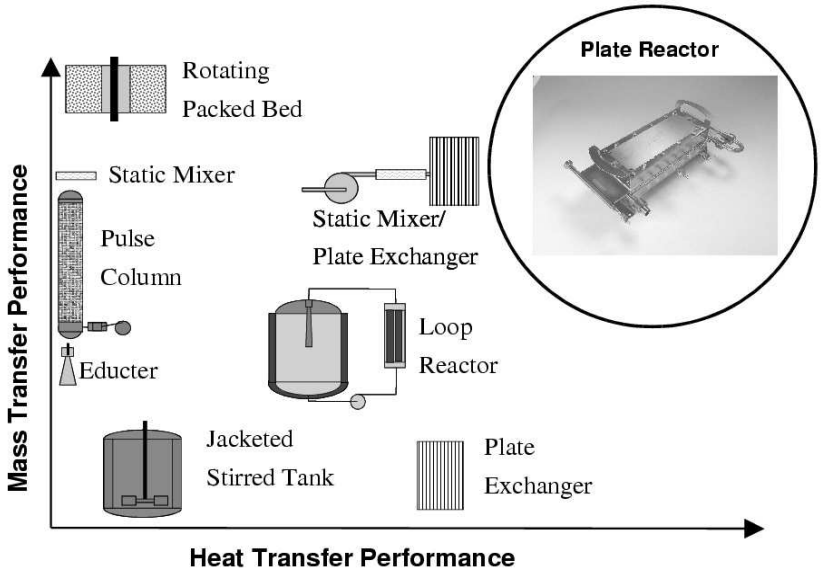

Figure 1.1 Heat transfer performance and mass transfer performance for the OPR and other kinds of chemical reactors. Courtesy of Alfa Laval AB.

fer capacity, have had limited success due to the poor micro-mixing conditions. In the 1990's, research on heat exchanger reactors, to overcome these problems, was started at the BHR Group Limited [Phillips *et al.*, 1997] and also at Alfa Laval AB [Nilsson and Sveider, 2000].

A new concept of heat exchange reactors, the Open Plate Reactor (OPR) is being developed by Alfa Laval AB within the ART project. It allows complex chemical reactions to be performed with a very accurate thermal control, by combing high heat transfer capacity with improved micro-mixing conditions. Therefore OPR appears particularly well suited for process intensification, as it allows at the same time an increase of reactant concentration and a reduction of solvent consumption. This leads to reduced need of down-stream separation, resulting in large savings in time and money. The improved heat transfer and mass transfer performances of the OPR, see Figure.1.1, means that the

OPR can replace larger conventional reactors, thus reducing plant size and investment costs.

However, to take full advantage of the flexibility and improved performance of the OPR, a new process control system is also required. The main purpose of the feedback control, besides safety, is to facilitate the handling of the process, that is, adjust input variables to compensate for uncertainties in valves, pumps, heat transfer coefficients and reaction kinetics. With the large number of input variables it is non-trivial how to manually adjust them to optimize performance, while maintaining safe operation. This thesis covers modeling, analysis and control design of the OPR and its cooling system.

1.2 Outline of the thesis

In Chapter 2, the OPR is described from a control engineering perspective and a nonlinear state-space model is derived from first principles, [Haugwitz and Hagander, 2004b]. Before a controller can be designed, suitable control variables are chosen based on dynamic and steady-state analysis in Chapter 3. In Chapter 4, the control objectives and structures are defined. A model predictive controller is designed to optimize the reaction conversion and maintain safe operating conditions inside the reactor. An extended Kalman filter is used for state and disturbance estimation, for example, to compensate for variations in feed concentrations. The suggested control system is verified in simulations with the nonlinear process model, [Haugwitz and Hagander, 2005].

To provide cooling or heating water to the OPR with desired temperature, a utility system has been designed by Alfa Laval AB. It is a general purpose hydraulic and thermodynamic system, but in this thesis it has been used as a cooling system and is therefore in the sequel referred to as either cooling system or utility system. In Chapter 5, the utility system and its control system are presented with experimental results. To control the water temperature, a mid-ranging control structure is used, which largely increases the operating range for the hydraulic equipment, [Haugwitz and Hagander, 2004a].

1.3 Publications

The thesis is based on the following publications:

Haugwitz, Staffan and Hagander, Per (2005): "Modeling and control of a novel heat exchange reactor; the Open Plate Reactor" Submitted to *Control Engineering Practice*

Haugwitz, Staffan and Hagander, Per (2005): "Process control of an Open Plate Reactor" In *Proceedings of IFAC World Congress*. Prague, Chech Rep. This paper received the IFAC Best Control Application Paper Award.

Haugwitz, Staffan and Hagander, Per (2004a): "Mid-ranging control of the cooling temperature for an Open Plate Reactor" In *Proceedings of Nordic Process Control Workshop*. Gothenburg, Sweden.

Haugwitz, Staffan and Hagander, Per (2004b): "Temperature control of a utility system for an Open Plate Reactor". In *Proceedings of Reglermöte*. Gothenburg, Sweden.

Other relevant publications are:

Haugwitz, Staffan; Karlsson, Maria; Velut, Stéphane and Hagander, Per (2005): "Anti-windup in Mid-ranging Control". Accepted to *the European Control Conference and the Conference on Decision and Control*. Sevilla, Spain.

Haugwitz, Staffan (2005): "Plattreaktorn öppnar nya vägar för kemiindustrin". Published on the web site of *Nationalencyklopedin*, Sweden, in connection to a course in Communication and Popular Science.

Haugwitz, Staffan (2003): "Modelling of Microturbine systems". In *Proceedings of European Control Conference*. Cambridge, UK.

2

Modeling

In this chapter, the design of the OPR is presented in Section 2.1 and the modeling of the OPR is described in Section 2.2.

Throughout the thesis, a simple exothermic reaction is considered. The substance A is the primary reactant and the substance B is the secondary reactant that is injected into the main flow of reactant A at multiple injection points along the reactor, see Figure 2.1.

$$A + B \rightarrow C + D \tag{2.1}$$

The desired product is substance C. Substance D is another product, with a constant stoichiometric relationship to C.

2.1 The Open Plate Reactor

The OPR is specifically designed to produce highly exothermic or endothermic and fast reactions. The aim is to safely produce the chemicals using highly concentrated reactant solutions. The main benefit is a reduced need of after-process separation to get products of high concentration.

The main new features of the OPR, needed to reach this objective, is the improved heat transfer capacity and the micro-mixing conditions inside the reactor.

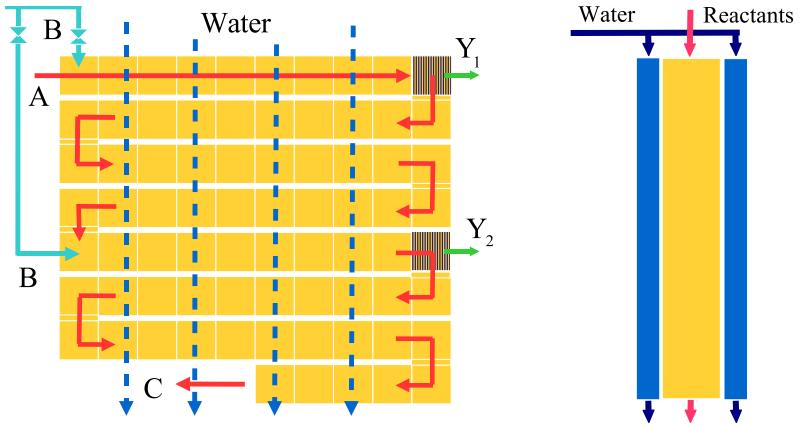

Figure 2.1 Left: A schematic of a few rows of a reactor plate. Reactant A is injected at top left and reactant B is injected at multiple sites along the reactor. Y_1 and Y_2 are internal temperature sensors used for process control and supervision. The cooling water flows from top to bottom in separate cooling plates. Right: The plate reactor seen from the side, with the reactor part in the middle and cooling plates on each side.

Process description of the OPR

The OPR is based on a modified plate heat exchanger design. It consists of reactor plates, inside which the reactants mix and react, and cooling plates, inside which cold water flows. There is one cooling plate on top of each reactor plate and one below.

In Figure 2.1 the OPR is shown from two different angles. The left figure illustrates the first rows of the reactor plate. Each row is divided into several cells. In the figure, 10 cells constitute one row. The primary reactant A flows into the reactor from the upper left inlet. Between the inlet and the outlet, the reactants are forced by inserts to flow in horizontal channels of changing directions. The flow inserts are specifically designed to enhance the micro-mixing and guarantee good heat transfer capacity, see Figure 2.2, and are patented in [Chopard, 2001] and [Chopard, 2002]. The dashed vertical lines of Figure 2.1 illustrate how the cooling water flows on each side to the reactor plate. The right figure in Figure 2.1 shows the OPR from the side with cooling

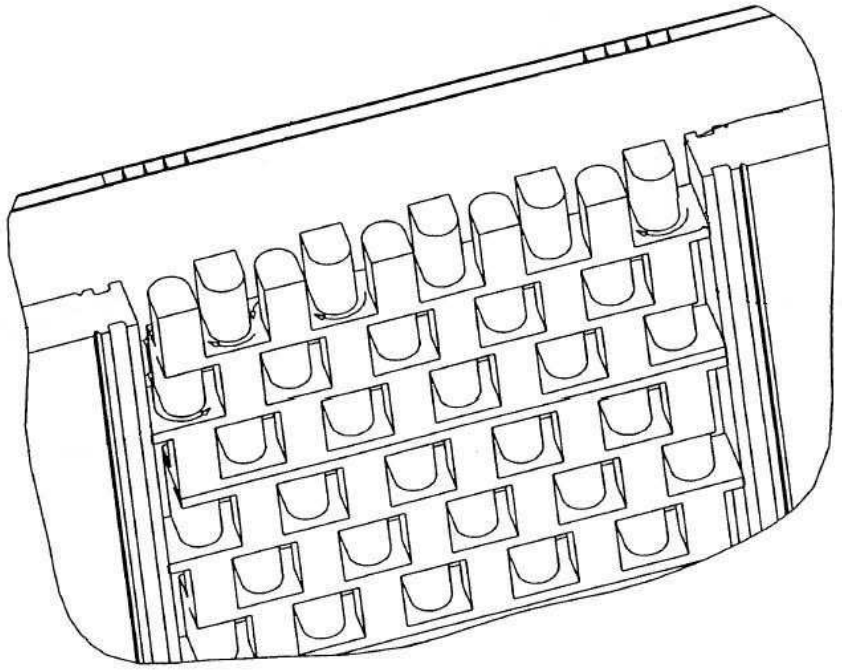

Figure 2.2 A drawing of the flow inserts and the flow channel shown in Figure 2.1,see also [Chopard, 2002]. Here the fluid enters from top right and the small arrows indicate the flow direction.

plates on each side of the reactor plate.

The design concept for the reactor allows for great flexibility in adapting the process for new reaction schemes. The type of inserts and the number of rows in the reactor plate can be adjusted to provide the residence time appropriate for the chosen reaction. If the reaction needs a catalyst, it can be mounted on the flow inserts. Reactant B can be injected in arbitrary places along the reactor, typically at the beginning and middle of the reactor. Temperature, pressure or conductivity sensors can be mounted inside the reactor, for example after each injection point, for process monitoring and control.

A test unit of the OPR is seen in Figure 2.3 and a lab-scale version

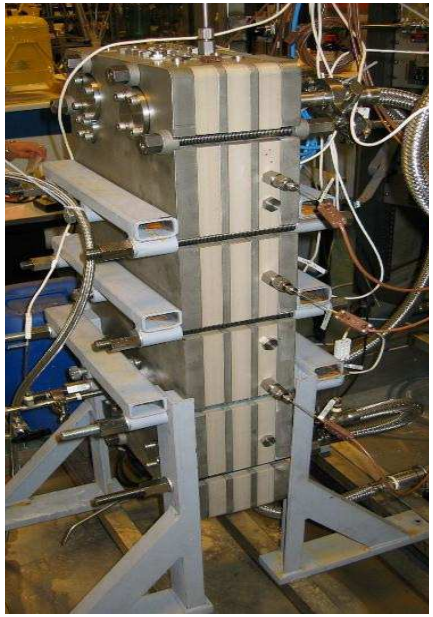

Figure 2.3 A test unit of the OPR with three plates connected in series. Note the temperature sensors along the side of one of the reactor plates. The thin cooling plates are mounted onto the reactor plates and are not visible in the photo. There are support plates between each cooling plate - reactor plate - cooling plate combination. Courtesy of Alfa Laval AB.

is seen in Figure 2.4.

Cooling

To further increase the flexibility of operation, it is possible to have separate cooling flows - with different temperatures - to cool selected parts of the reactor. The cooling plates are then divided into several compartments, each having an individual cooling inlet temperature. For some reactions it may even be beneficial to heat the last section of the OPR to further increase the conversion. However, for most reactions and for the one in this thesis, it is adequate to use the same water to cool an entire reactor plate.

While the cooling plates on each side of the reactor plate have verti-

Figure 2.4 A lab-scale version of the OPR for initial testing of new reaction schemes. Courtesy of Alfa Laval AB.

cal flow channels, reactor channels are horizontal, giving a cross-flow heat exchange pattern. However, the general flow direction of the reactor flow is vertical, so the heat exchange pattern can be modelled as concurrent.

The cooling water comes from a utility system, described in Chapter 5, where a temperature controller ensures that the water has the desired temperature when entering the OPR.

Reactions

Several different types of chemical reactions have been tested in the OPR, such as single liquid-phase exothermic irreversible reactions, single liquid-phase exothermic reversible reactions and liquid/liquid exothermic reactions for un-miscible flows (cf. oil and water). There have also been tests on liquid/gas reactions. The focus in this thesis is on reactor modelling and process control, so in the sequel a single

liquid-phase exothermic irreversible reaction is being studied; oxidation of thiosulfate by hydrogen peroxide, a fast and exothermic reaction.

$$2Na_2S_2O_3 + 4H_2O_2 \rightarrow Na_2S_3O_6 + Na_2SO_4 + 4H_2O \tag{2.2}$$

The kinetic reaction parameters are $k^0 = 2 \cdot 10^{10}$ L/(mol s), $E_a = 68200$ J/mol and $\Delta H = -586000$ J/mol thiosulfate, which are used in Eq. (2.7).

2.2 Modeling

A model of the OPR can be derived from first principles, with equations for heat transfer, reaction kinetics, mass, energy and chemical balances, see for example [Thomas, 1999]. A good introduction to chemical reaction engineering can be found in [Fogler, 1992].

The multiple consecutive horizontal channels inside the OPR in Figure 2.1, can be approximated as a continuous tubular reactor with injections of reactant B along the reactor.

Experiments performed at Chalmers, see [Bouaifi *et al.*, 2004], [Andersson *et al.*, 2004a], [Bouaifi and Andersson, 2004], [Andersson *et al.*, 2004b], have shown that perfect mixing conditions are achieved already after a few cells, that is, a fraction of a row. This implies that the Arrhenius law can be used for modeling the reaction kinetics.

Experiments performed at Alfa Laval have shown that the flow inside the reactor can be viewed as almost plug flow. This means that diffusion terms in the length axis of the reactor can be neglected compared to convection terms. It also implies that there are no significant dead zones or stagnant zones.

Partial Differential Equations

From first principles, a partial differential equation (PDE) for an infinitesimal element of the flow channel is derived. The energy balance in a small element of length ∂z without any reactant injections is stated as

$$\rho c_p \frac{\partial T_r}{\partial t} = -\rho c_p v_r \frac{\partial T_r}{\partial z} + h\frac{L_z}{A_z}(T_c - T_r) + \Delta H_r r(c, T_r) \tag{2.3}$$

where T_r and T_c are the temperatures in the reactor element and the adjacent cooling element, respectively. L_z is the circumference and A_z is the cross-section area of the flow channel. The heat transfer coefficient is denoted by h and v_r is the fluid velocity through the reactor element. ΔH_r is the reaction energy term. The reaction rate is denoted by $r(c, T_r)$ and depends on the concentrations and temperatures. The temperatures of the cooling water and the concentrations of each substance are described by similar PDE's.

Discretization

To simplify analysis of the PDE, which is an infinite dimensional system, the spatial derivative is approximated, using a first order backward difference method, as a finite system of ordinary differential equations (ODE). The model is discretized using n elements of equal size, where n can be a design parameter and may then be chosen such that the numerical dispersion approximates the actual dispersion of the reactor. More details of numerical methods can be found in [Wouwer *et al.*, 2004; Renou *et al.*, 2003]. The discretization can be viewed as connecting n perfectly mixed tanks in series. This implies that in each element we assume homogeneous properties, such as temperature and concentrations.

Balance Equations

The states of the model in each element are the temperatures of the reactor fluid, the cooling water and the concentrations of the reactants A and B and the product C. For the k:th element, in which reactant B is injected, $1 < k < n$, the equations for energy and chemical balance can be written as

$$\rho c_p V_r \frac{dT_r[k]}{dt} = \rho c_p \left(q_r[k-1]T_r[k-1] - q_r[k]T_r[k]\right) + hA_{heat}(T_c[k] - T_r[k]) + \Delta H_r r[k] V_r \quad (2.4)$$

$$\rho c_p V_c \frac{dT_c[k]}{dt} = \rho c_p q_c (T_c[k-1] - T_c[k]) - hA_{heat}(T_c[k] - T_r[k]) \quad (2.5)$$

$$V_r \frac{dc_B[k]}{dt} = q_r[k-1]c_B[k-1] - q_r[k]c_B[k] + s_{t,B} V_r r(c, T_r)[k] + q_{feedB,k} c_{feedB,k} \quad (2.6)$$

where T_r and T_c are the temperatures in the reactor and in the cooling water. The variables q_r and q_c are the flows through the reactor and the cooling plates respectively. ΔH_r is the reaction energy term, r is the reaction rate, $s_{t,B}$ is the stoichiometric coefficient for reactant B. h and A_{heat} are the heat transfer coefficient and area, respectively. The heat transfer coefficient h depends mainly on the flow rate and since the OPR is studied for constant flow rates in the thesis, h is also approximated as a constant. V_r and V_c are the volumes of one element of the reactor fluid and the cooling fluid. Constant values for the density ρ and heat capacity c_p are used. For the OPR, the thermal inertia of the water and the chemicals dominate over that for the metal, which is therefore not included in the model. The subscript $feedB,k$ denotes the flow and concentration of reactant B that is injected into element k. There are similar equations for the other substances A and C. The index k refers to the value of that property in element k, and $k-1$ refers to the value in the previous element. In this thesis we study a liquid/liquid irreversible exothermic reaction of second order. As stated earlier, experiments have shown that good micro-mixing is achieved in the OPR. The reaction term $r[k]$ in element k can then be described by the Arrhenius law

$$r(c, T_r)[k] = k_0 e^{\frac{-E_a}{RT_r[k]}} c_A[k] c_B[k] \quad (2.7)$$

where k_0 is the pre-exponential factor, E_a is the activation energy, R is the universal gas constant and c_A and c_B are the reactant concentrations in element k. Note that the derived model is highly nonlinear

due to the temperature influence on the reaction rate and the product of the two reactant concentrations.

Model errors

To reduce computational complexity it is desirable to use lower order models by using fewer elements in the discretization of the process. If very few elements are used, when discretizing the PDE, the homogeneous temperature assumption in each element implies that a large section of the actual reactor has the same temperature. This may result in large model errors due to averaging, see Figure 2.5. There is a large difference in the maximum temperature predicted by the models, depending on the choice of n. This is a result of the nonlinear temperature-dependent reaction rates. The model errors are important to consider, since the errors may lead to violation of temperature constraints.

In general all elements are of equal size, but by using smaller elements around the temperature maxima and where the temperature gradient is large, the resolution of the temperature profile can be significantly improved. This can be compared to standard finite element modeling, where the grid pattern is refined at interesting points and more coarse at other points. However, then you have to know in advance the locations of the temperature maxima and they may change during transients or due to disturbances. An even better, but more complex solution, is to use a moving mesh method that changes the discretization based on error analysis, see [Liu, 2005]. Another alternative is to utilize the PDE's directly in the control design, see for example [Christofides, 2001] or [Shang *et al.*, 2005].

There can also be parameter errors, in terms of uncertain reaction kinetics, heat transfer coefficients and inlet flow disturbances, such as variations in feed concentrations.

Implementation

The model has been implemented in the Modelica language and simulated in Dymola, see [Modelica Association, 2000] and [Dynasim, 2001]. The model has been verified against experimental data from Alfa Laval AB.

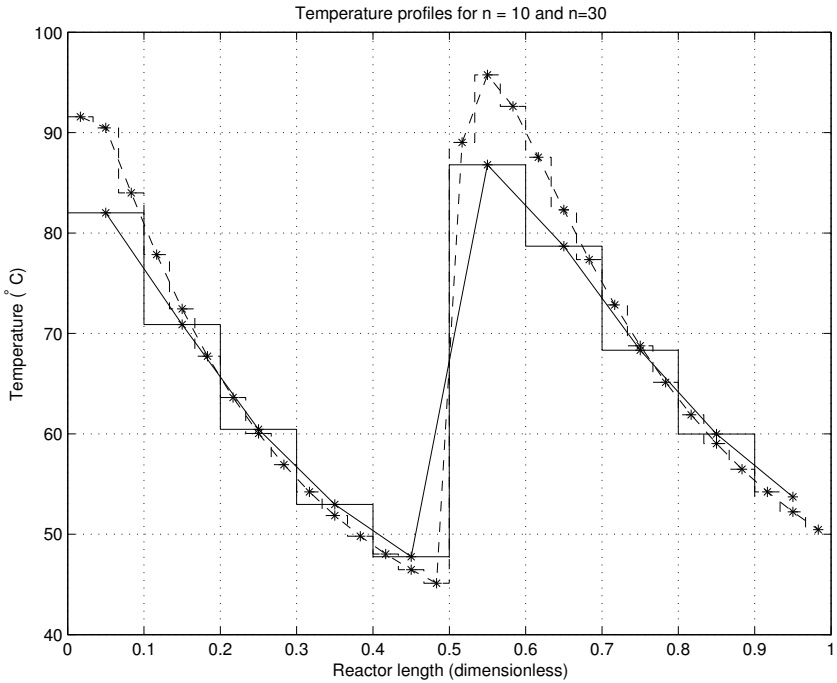

Figure 2.5 Steady-state temperature profiles for the OPR with reactant injections in two points. If the OPR is modelled using $n = 30$ elements (dashed), the resolution of the temperature profile is improved, compared to $n = 10$ (solid). Note that the OPR model assumes homogeneous temperature in each model element.

3

Process design and operation

In the previous section, we presented the OPR and derived a nonlinear state-space model from first principles. Given a specific reaction, it is a non-trivial task to design the OPR process in terms of physical size, materials, flows, operating points and choice of control signals. The design of the physical parameters of the OPR and the variables closely linked to the physical size, such as flow rate through the reactor is beyond the scope of this thesis. In this section we will, given the physical size of the OPR, suggest ways how it can be operated to maximize its performance and safety.

3.1 Process design and operation objectives

Process design

The overall objective of the OPR is to produce high quality chemicals in an efficient way at a low cost. Traditionally the development of a chemical process starts with the design phase and after that the control design is made for the given physical data and choice of operating point. In this project, the design of the process and its control system has been developed in parallel. The advantage is that already at an early stage, a full dynamic analysis is made and possible control strategies are evaluated. Conclusions from simulations can then be used to refine the

process design, which may improve the performance during operation.

With the flexible configuration of the OPR described in Section 2, there are many degrees of freedom when determining the process design and how to control it. When a specific reaction is to be produced, the following properties have to be determined through hydraulic, thermodynamic and chemical reaction analyses.

- Determine which of the reactants that should be the primary reactant that constitutes the main flow and the secondary reactant that is injected along the reactor.
- Determine the appropriate length of the reactor channel, so the reaction is completed before the outlet.
- Determine the outlet flow rate from the reactor and the internal pressure inside the reactor.
- Determine the optimal number and location of the reactant injections.
- Determine the optimal distribution of the reactant, that is, how much of the reactant should be injected in each injection point.
- Determine the appropriate cooling medium, usually water and its desired inlet temperature and flow rate.
- Determine if the reactants can be injected at ambient temperature or they need to be heated to facilitate ignition of the reaction.
- Determine the number and location of the internal sensors needed for good process control and monitoring.
- Determine if a catalyst is needed.

All these decisions depend on each other, which makes the process design a very difficult procedure to optimize. For example the reactor would be better utilized the more injection points there are, but due to hydraulic and micro-mixing conditions, there is a lower limit on the flow rate to be injected. In the effort of improving the performance, the process design and control design tend to be more and more connected. The physical design of the OPR will have a major impact on to what extent the reactor needs to be controlled and also how the reactor

can be controlled. If for example the OPR is designed to have a very long residence time, the reaction will easily be completed even if the reactor temperature is moderate. However, process intensification demands more compact solutions and the reaction should be completed with as short flow time as possible. It is then necessary to increase the reaction rate by all means possible, for example increasing the temperature as high as possible and introducing new inserts for improved micro-mixing. The process design properties above are often determined by steady-state optimizations of a very detailed nonlinear process model.

Objectives and process limitations

In the sequel we will assume that the physical design of the OPR has been fixed, as well as the total feed flow rate. In this thesis, we focus on how we should control the process to improve its performance, while maintaining safe operation. The main benefit of using feedback control is that it will facilitate the handling of the process, that is, adjusting the input variables to compensate for uncertainties in the valves, pumps, heat transfer coefficients and reaction kinetics.

The main objective of operation is to have complete conversion of the reactants A and B to the desired product C. The focus is then to maximize the outlet concentration of C, but without having too much excess of either reactant. The conversion, γ, can be defined as the ratio between how much product that was formed and how much that could have been formed.

$$\gamma = \frac{c_C}{c_C + c_A} \tag{3.1}$$

where c are the concentrations at the reactor outlet. If all reactant has been converted into product, $\gamma = 1$, also viewed as 100%. Note that the conversion is a nonlinear function of the concentrations.

100% conversion is only possible in a reactor of infinite length. For industrial reactors, one of the main limitations is the temperature constraint. The material inside the reactor, possible by-product formation or the boiling point for the given reactor pressure, all these factors lead to the definition of a maximum temperature allowed inside the OPR. To avoid excessive temperatures, the OPR is cooled with water. The

limitation in that case is the lowest available inlet temperature of the cooling water, typically taken from a nearby river or lake.

In some applications it may also be desirable to have a certain outlet temperature of the product, to improve conditions for downstream processing.

In the next sections, we will discuss the different input variables and how they can be used to control the conversion of the OPR, thus improving the performance of the process.

3.2 Input and output variables of the OPR

In Figure 3.1 the input and output variables for the OPR are shown. In this figure and in the sequel of the thesis we will consider the case when there are two injection points used, one in the beginning and one in the middle of the reactor. The reactant flows are often also called feeds, such as feed concentration, to distinguish between the properties of the inlet flows and those inside the reactor. All temperatures and flow rates of the feeds are measured as well as temperatures inside the reactor. Online measurements of the concentrations are, however, only available in special cases.

An input variable specific for the OPR is how we choose to inject the reactants. One reactant is chosen to be the primary reactant A and the other reactant B is the secondary reactant. Reactant B is now injected at multiple injection points along the side to the OPR. From the initial process design, the flow rates through the reactor have been determined. However, one degree of freedom is left, that is how the reactant B flow should be distributed between the different injection points. For an exothermic reaction, the distribution of the reactant B flow will have a major impact on the temperatures inside the OPR, as shown in Section 3.3

3.3 Steady-state and dynamics analyses of the OPR

In this section we will use the nonlinear model derived in Chapter 2, to improve our process knowledge of the OPR. It will help us in our

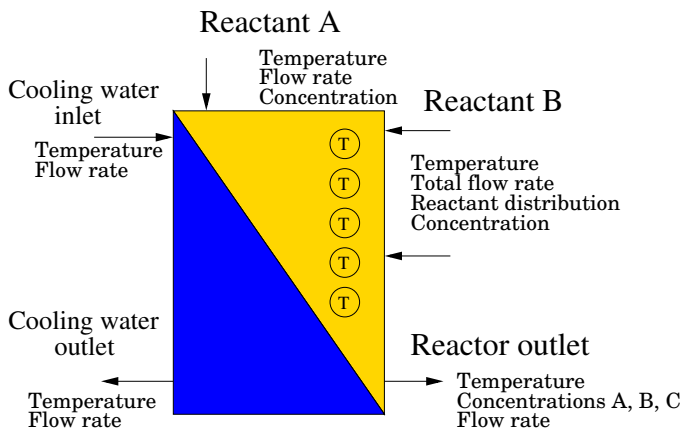

Figure 3.1 The Open Plate Reactor as a schematic heat exchanger with reactions on one side and cooling water on the other side. There are multiple injection sites and internal temperature transmitters are distributed along the reactor side.

choice of suitable control variables from the available input variables shown in Figure 3.1. The exothermic reaction used in the simulations is oxidation of thiosulfate by hydrogen peroxide, see Eq (2.2). We will start with a steady-state analysis, to get an overview of the effect the different input variables have on the reactor. The simulations shown in this chapter are for illustrative purposes only. Temperatures above 100° C are possible, only because the nonlinear model does not consider boiling conditions and pressure.

Steady-state analysis

In Figure 3.2 the steady-state temperature and conversion profiles along the reactor are plotted. Two injection sites are used in this example, one at the inlet and one in the middle of the reactor. There is a temperature maximum after each injection point, which is typical for exothermic reactions. In this section we will elaborate how these profiles vary with different values of the following input variables; *reactant B injection distribution, cooling inlet temperature, reactant inlet temperature* and *reactant inlet concentration*. All other input variables are assumed to be constant. The simulations are based on the nonlin-

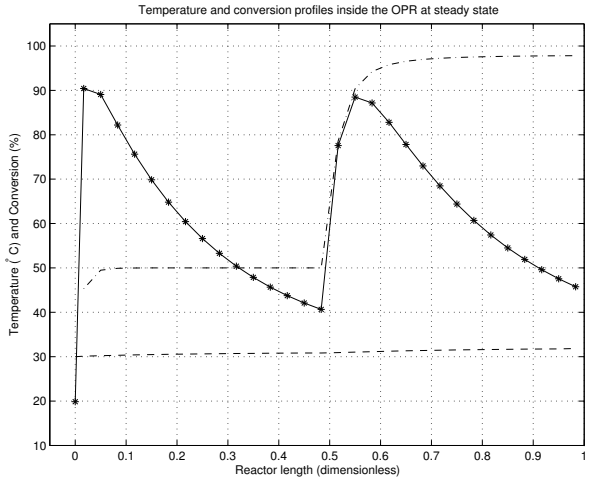

Figure 3.2 Simulated temperature (solid), conversion (dash-dot) and cooling temperature profile (dashed) along the OPR with reactant injections at two sites resulting in two temperature maxima at $T = 90.4$ and 88.5°C.

ear model in Chapter 2, but the model does not consider boiling effects, so the figures in this section should only be considered as simple illustrations of the impact of each input variable on the OPR.

Nominal case. The nominal case is shown in Figure 3.2 using the following values of the input variables. The reactant injection flow distribution is 0.50, i.e. 50% of the reactant B flow is injected at the inlet and 50% in the middle of the reactor. The cooling inlet temperature is 30°C. The reactant inlet temperatures are 20°C for both reactants and the nominal reactant concentrations c_A^0 and c_B^0 are used. The nonlinear model from Chapter 2 is used and the OPR is discretized into $n = 30$ elements.

Together this set of input variables leads to two temperature maxima of $T = 90.4$°C and 88.5°C. The conversion of reactant A reaches 50% after the first injection, due to the surplus of reactant A in the first half of the OPR. After the second injection, the conversion reaches 97.8% at the outlet of the reactor, which constitutes the main performance variable of the reactor.

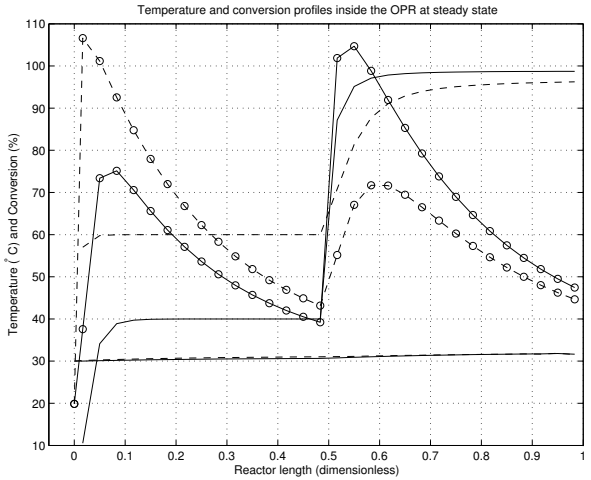

Figure 3.3 Simulated temperature, conversion and cooling temperature profile along the OPR when the distribution of reactant B is 40/60 (solid) compared to the case 60/40 (dashed).

Changes in the reactant injection distribution. In Figure 3.3, the distribution of the reactant B has been varied, from 40/60 (40 % is injected in the first injection point) to 60/40. The figure shows the close relationship between the injection distribution and heat release distribution, causing a significant difference in the temperature profiles. The conversion is slightly higher for the 40/60 case, since the larger second injection leads to higher temperature there, thus increasing the reaction rate. The total amount of heat released is proportional to the conversion.

Changes in the cooling temperature. In Figure 3.4, the cooling inlet temperature has been varied, from 20°C to 40°C. Here we can see that the change in T_{cool} has a limited influence on the first temperature maximum. The conversion after the first injection point is therefore almost the same. The main effect is instead on the second temperature maximum. With more cooling, the reaction rate is slower in the second part of the reactor, thus leading to a lower conversion. Note that the cooling power, the transfered power out from the reactor, is a linear

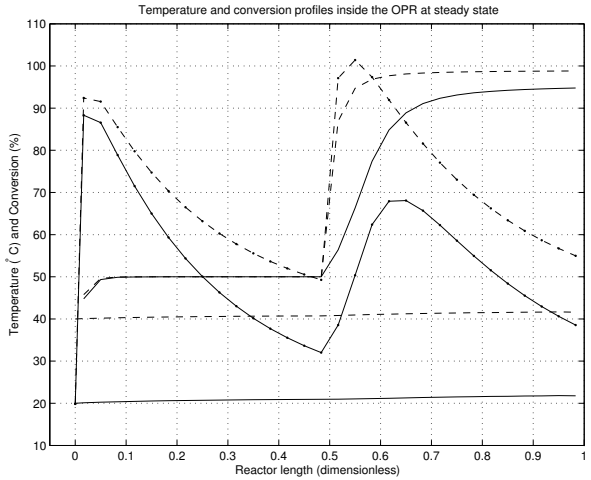

Figure 3.4 Simulated temperature, conversion and cooling temperature profile along the OPR when the cooling inlet temperature is 20°C (solid) compared to the case 40°C (dashed).

function of the temperature difference ($T_{reac} - T_{cool}$), so by manipulating the cooling temperature, it is easy to control the reactor temperature around the second temperature maximum.

Changes in the cooling flow rate. In Figure 3.5, the cooling flow rate has been varied, from q_{cool} to $0.05 \cdot q_{cool}$. The heat transfer from the reactor is proportional to the temperature difference between the reactor fluid and the water. If a low cooling flow rate is used, $0.05 \cdot q_{cool}$, the cooling water is significantly heated by the reactor and the temperature difference decreases along the reactor. To increase the cooling, a higher flow rate is used, $0.2 \cdot q_{cool}$. More water transfers the reactor heat and the temperature difference increases. The third case is q_{cool}. Then the flow rate is so high that the temperature of the cooling water remains roughly constant. After that there is no use of further increasing the flow rate since the temperature difference and the heat transfer remains constant. The use of varying flow rate as a control variable saturates when the gain from the flow rate change to temperature change approaches to zero.

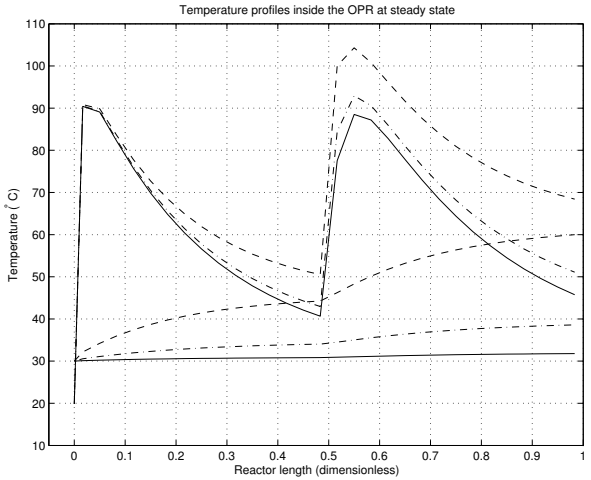

Figure 3.5 Simulated reactor temperature (the upper curves) and cooling temperature (the lower curves) profiles along the OPR when the cooling flow rate varies from q_{cool} (solid), $0.2 \cdot q_{cool}$ (dash-dot) to $0.05 \cdot q_{cool}$ (dashed).

Changes in the feed temperature. In Figure 3.6, the inlet temperatures of the two reactants are 10°C and 30°C, respectively. The change in T_{feed} has a major impact on the first temperature maximum and less on the second maximum. The feed temperature can therefore be useful to control the temperatures in the beginning of the OPR. Note that the conversion is the same for the two cases after one fifth of the reactor length.

Discussion. A change in cooling flow rate q_{cool} may give a similar effect as in Figure 3.4, but without the simple linear relation between input variable and cooling power, see further discussion in Section 3.5. An increase in the feed concentrations of A and B would lead to an increase in total heat released and therefore also to increased temperatures in both maxima. Note that the change in the injection distribution has effects on *both* maxima, compared to the changes in cooling or feed temperature, where only one of the maxima is effected.

All figures show that increased temperature leads to increased conversion, for this specific reaction. To maximize the utilization of the re-

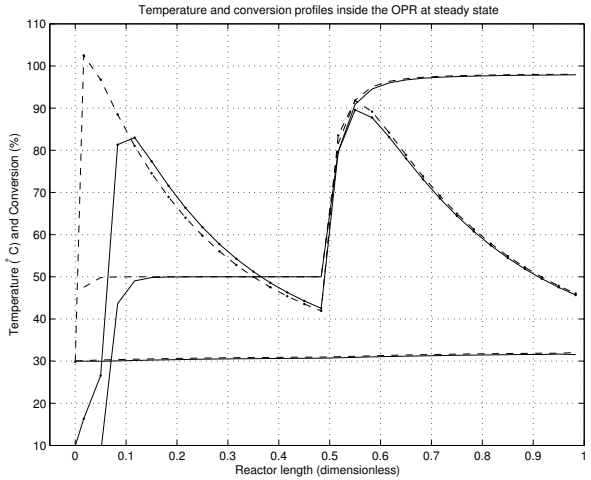

Figure 3.6 Simulated temperature, conversion and cooling temperature profile along the OPR when the reactant inlet temperatures are 10°C (solid) compared to the case 30°C (dashed).

actor, the input variables should therefore be chosen in such a way that the two temperature maxima are both at the highest possible value at which it is safe to operate. This requires control variables that can influence the temperature along the entire reactor and the amount of heat transfered from the reactor. Based on these reasons, using only one of the input variables presented above is not adequate. Instead at least two of them should be used for control, based on the steady-state analysis.

Dynamic analysis of the OPR

For control purposes it is critical to have a thorough knowledge of the dynamics of the process. It is not enough to study the steady state plots from previous section. Especially for exothermic reactions that may lead to unstable processes. It is then vital to have control variables with fast actuator dynamics to allow stabilizing control actions, see for example [Stein, 2003].

The main dynamics of the OPR are the fast chemical reaction ki-

Table 3.1 The changes of input variables during simulation

Time (s)	Input change
100	reactant distribution from 0.4 to 0.6
200	reactant distribution from 0.6 to 0.5
300	cooling inlet temperature from 30°C to 20°C
400	cooling inlet temperature from 20°C to 40°C
500	cooling inlet temperature from 40°C to 30°C
600	reactant feed temperature from 20°C to 10°C
700	reactant feed temperature from 10°C to 30°C
800	reactant feed temperature from 30°C to 20°C
900	reactant feed concentration from 100 % to 110 %
1000	reactant feed concentration from 110 % to 100 %

netics and the slower heat transfer dynamics. In addition there is a significant flow time from the inlet to the outlet of the process, called the residence time.

The reaction kinetics can differ many orders of magnitude from one reaction to another. The use of the OPR is generally aimed at fast reactions, since slower reactions would require long reactor length to have complete reaction.

To visualize the dynamics of the process and the different effects the input variables have on the output variables of the OPR, the simulation scenario in Table 3.1 is considered. We use the nonlinear model from Chapter 2 and use $n = 30$ elements to represent the OPR. Also in these simulations, there are two reactant injections, one at the inlet and one in the midsection, element 1 and 16 respectively.

There is a very closely coupled relation between temperature and concentrations, see Figure 3.7. An increase in reactor temperature leads to increased reaction rate and therefore also increased heat generation, which leads to even higher temperatures. If the concentrations are increased, this also increase the reaction rate and therefore also the temperature.

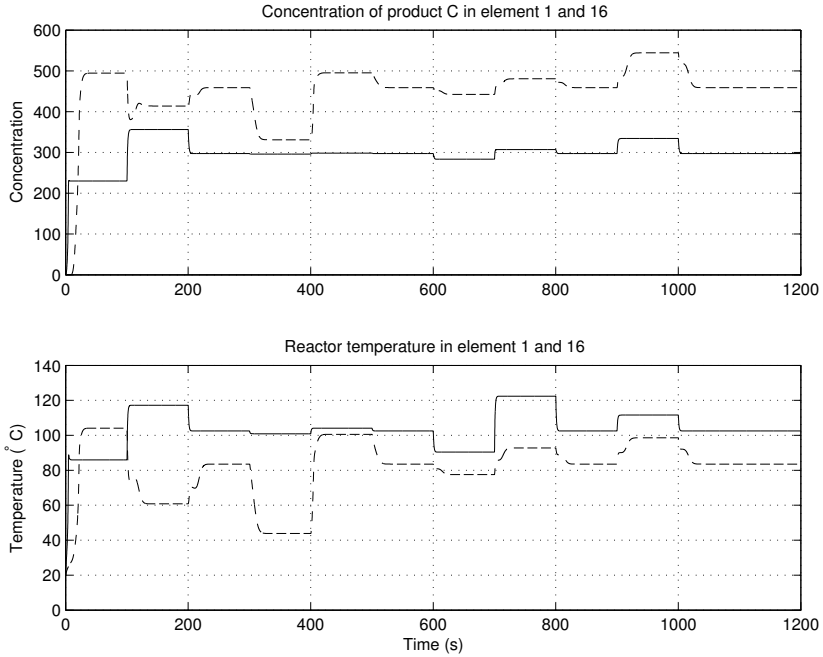

Figure 3.7 Concentration of product C and reactor temperatures in elements 1 (solid) and 16 (dashed) during simulation according to Table 3.1.

Note the small effect from the increase in cooling temperature to the reactor temperature in element 1. Compare this to the much larger effect on the reactor temperature in element 16, with corresponding increase in product concentration. The reactor temperature in element 16 experiences a small upset at $T = 120$ s. The warmer fluid from the beginning of the reactor has then reached the midsection and effects the temperature there. The same effect can be seen after every step change, where the two reactor temperatures change in opposite directions.

For the specific reaction kinetics, it can be seen in Figure 3.7 that the time constant for the dynamics of the product concentration at time $t = 100$ s is roughly 1.1 seconds. For the thermal changes the estima-

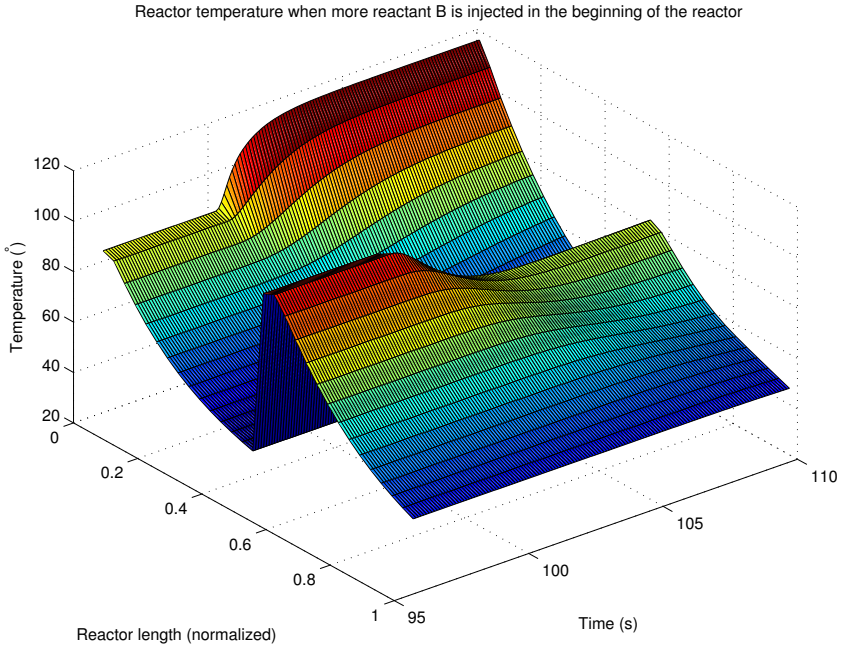

Figure 3.8 3D image of the reactor temperature when the reactant injection distribution is changed so that more reactant B is injected in the first injection site. Reactor length 0 represents the inlet of the OPR and 1 the outlet.

tion of the time constant is less straight forward, due to the flow time of the cooling water and the reactor flow and the nonlinear relations between temperature and reaction kinetics. The reactor temperature in the different elements have a time constant from 1.2 to 6 seconds, depending on the sensor location. It might appear surprisingly fast, but modern high-efficient plate heat exchangers have a very fast dynamic response, due to low metal mass compared to the vast heat transfer areas.

The residence time, the flow time from inlet to outlet, of 30 seconds contributes significantly to the reactor dynamics, especially if an outlet variable is to be controlled with an input variable of the reactor. The flow time for the cooling water is much shorter, 0.5 - 6 seconds

depending on the flow rate. This implies that a change in any reactor outlet variable is easier carried out by varying the cooling than using a reactor inlet variable.

To further illustrate the time and spatial dependency of this process, Figure 3.8 shows the entire temperature profile for the time interval $t = 95 - 110$ s from Figure 3.7. The x-axis (on the left) is the normalized reactor length from 0 to 1, the y-axis (on the right) is the simulated time and the z-axis is the reactor temperature. We clearly see the simultaneous change in the two temperature maxima, when more reactant is injected in the first element and less amount in the midsection.

Stability of the open loop process

Exothermic reactions inside the OPR may lead to an unstable open loop system. The OPR can be viewed as a tubular reactor, which is a distributed parameter system described by partial differential equations. The infinite dimensionality of the PDE's makes the stability analysis much more difficult than for a finite dimensional system like a tank reactor. In [Winkin *et al.*, 2000] a dynamic analysis of tubular reactors is presented within the infinite-dimensional framework. Conditions for observability, controllability and stability are derived.

A simpler, but less exact way to view stability of the OPR is to study the amount of heat removed by the cooling water and the heat released from the reaction as functions of the actual reactor temperature, see for example [Shinskey, 1996]. In this approach, the tubular reactor is discretized into several smaller elements. The energy balance for one discretized element of the reactor gives is

$$\rho c_p V \frac{dT}{dt} = -hA(T_{reac} - T_{cool}) - q\rho c_p(T_{reac} - T_{feed}) + r(T, C)V\Delta H \tag{3.2}$$

The first two terms on the right hand side are cooling terms and the last term on the right hand side is releasing heat. Note that the cooling terms are linear in temperature, whereas the heat release is nonlinear, due to the reaction rate and the finite amount of available chemicals. There is a maximum of heat release when 100% of the reactants have converted into products.

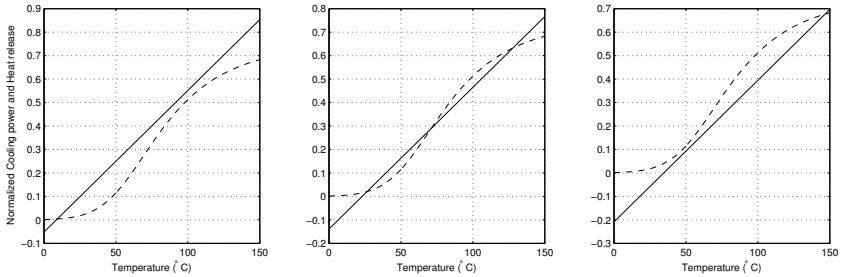

Figure 3.9 Stability analysis of open loop process with exothermic reaction for a discretized element of the OPR. Different cooling temperatures. Left: $T_{cool} = 8°$ C, Middle: $T_{cool} = 23°$ C, Right: $T_{cool} = 35°$ C. The cooling power (solid) compared to the reaction heat released (dashed) as functions of the reactor temperature.

In figure 3.9, the terms are plotted for the first discretized element in the OPR model with $n = 100$ to provide accurate resolution of the temperature profile. The temperature and concentrations are homogeneous within the discretized element. For the three plots, different inlet cooling temperature are used; $T_{cool} = 8, 23$ and 35°C for the left, middle and right plot respectively.

Each point where the cooling line (solid) crosses the heat release curve (dashed), is an equilibrium point. In Figure 3.9, we see that the left plot has one, the middle has three and the right plot has one equilibrium point.

Consider operating at the unstable equilibrium point in the middle point, if the temperature is slightly increased, the heat released will be greater than the cooling power and the temperature will continue to increase until the process converges to the upper stable equilibrium point. However in many cases the cooling line and the heat release curve only intersect in one point, which results in one stable equilibrium point.

In the left plot in Figure 3.9, the cooling power is so large with $T_{cool} = 8$°C that the process stays at a low temperature equilibrium point. In the right plot, cooling power is small with $T_{cool} = 35$°C, so a much higher temperature equilibrium is achieved. Similarly, if we change the feed concentration or the feed temperature, the dashed heat

release curve will be different and a similar analysis can be made.

This rough analysis is only valid for this specific element. The OPR is approximated as many elements in series. It is then vital to analyse the situation in all elements, especially during transients. By studying Figure 3.9, we see that the stability depends on many factors, such as feed concentration, feed temperature and cooling temperature, which helps us understand how to control the OPR.

The possibility of multiple equilibrium points, means that the state trajectory from initial conditions to the desired operating point may be non-trivial. The transfer from one equilibrium point to another can be seen as *ignition* of the reactor, which is critical during the start-up sequence.

3.4 Operating modes

The OPR is a continuous reactor, and is therefore supposed to be in operation 24 hours a day, seven days a week. However, there are a few discrete operational modes connected to the start-up and shutdown procedures. Even though they only constitute a negligible fraction of the operational time, these procedures may be critical for a successful operation, especially the start-up. In this section, the three different operating modes of the OPR will be briefly described and the type of control needed in each operating mode, see Figure 3.10. The main focus in this thesis is on nominal control, after initial transient from rest, the controller should manipulate input variables to optimize conversion and keep the reactor temperatures below some given safety limit.

Start-up control mode

The start-up phase will be very different depending on the chemical reaction to be produced. In some cases it will be straightforward, but in many cases it will probably be the most difficult part of operation for the OPR. The aim is to safely bring the process from initial conditions to the desired steady-state of nominal operation. The main challenge is that some reactions are difficult to start, also called to ignite, and after ignition the exothermic reaction needs quickly to be cooled to prevent thermal runaways. During the start-up, there will be transients in

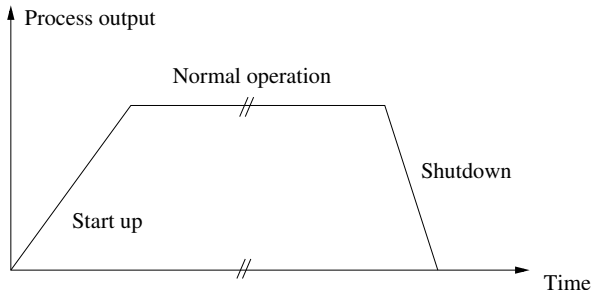

Figure 3.10 A schematic figure of a typical sequence of operation

temperature, flow rates and concentrations that the control system has to deal with. The process will during this period have a strongly nonlinear behavior, which any model-based control has to consider.

The start-up phase of the production should therefore be carefully planned for each specific reaction and for each choice of operating conditions, e.g. inlet concentrations and inlet temperatures. The start-up transients and the ignition of the reaction will mainly depend on the feed concentrations and feed temperatures. If the feed temperature or the feed concentrations are too low, the reaction rate will be very low and only a minor fraction of the reactant will be consumed, releasing small amounts of heat. This correspond to a lower equilibrium point. If the temperature or the concentrations are increased the reaction rate will increase, which will give additional heat release and increased temperature. The process will then converge to another equilibrium point with higher temperature.

The most simple start-up procedure can be the following:

1. Start cooling with water of very low temperature.
2. Start the flow of reactant A.
3. Slowly ramp up the flow of reactant B using a fixed reactant injection distribution.
4. Slowly ramp up the cooling temperature to a nominal operating point.

5. When the process has entered the nominal operating point and the reaction has been ignited successfully, the start-up phase is ended and the controller is switched to nominal operating mode.
6. During start-up the outflow from the reactor goes into a waste tank. When the product obtains the required quality, a valve is switched that allows the outlet flow of the OPR to continue downstream for further processing.

The main control objective during start-up may not be to maximize conversion, but to keep the reactor temperature below a certain safety limit.

To control the process during the start-up transients, the cooling inlet temperature may be the primary manipulated variable. An additional control variable during start-up can be the feed inlet temperature. To promote ignition, the feed inlet temperature can be temporarily raised. Normally the reaction scheme should be designed so the reaction is able to ignite without additional heating, since it requires more complex equipment.

Nominal control mode

In the nominal control mode, the main objectives of the control system are to ensure safe production by keeping the reactor temperature below some given safety limit and to achieve optimal conditions inside the OPR, which lead to maximum conversion. The operating point at which this is achieved is not exactly known in advance. Off-line calculations can give initial suggestions, but process uncertainties may result in sub-optimal conditions or lead to reactor temperatures that are dangerously high and cause unnecessary process shutdowns. Instead of trial-and-error open loop control, feedback control can adjust the input variables to compensate for these uncertainties in for example valves and pumps characteristics, heat transfer coefficients or reaction kinetics. Since the OPR will spend most of if its time in this mode, it is crucial that the chosen operating point gives good performance. Even a small increase in conversion or productivity will over time give large effects on the economy of the process.

The control system should also prevent any disturbances outside the OPR to affect the input flows to the OPR, for example by feed forward control or integral action through disturbance estimation.

Shutdown control mode

The shutdown mode is activated when the production should be halted. It should be an orderly and safe shutdown, so that production can be restarted easily. Emergency shutdown is a different procedure, that will not be discussed here. The shutdown control sequence will have to be designed specifically for each reaction and reactants. Normally for an exothermic reaction it would start by closing all the inlet valves of the secondary reactant and then after some time also close the inlet valve of the primary reactant. When the flow rate of the secondary reactant is stopped, a magnetic valve should be switched so that the remaining product in the OPR flows into a buffer tank instead of further down the production line. Depending on the reactants used, the system may need to be rinsed before restart.

3.5 Choice of control signals

In previous sections, we have presented a nonlinear model of the OPR, steady-state and dynamic analyzes, discussed stability issues of the reactor and different control modes. In this section we will combine this information to choose suitable control signals for the nominal control mode.

The performance of the OPR depends directly on the outlet concentrations, and from the equations derived in Chapter 2, we see that the concentrations depend on the temperatures along the reactor. The main focus is then to choose control signals that give accurate, fast and flexible control of the temperatures inside the reactor.

Traditionally, the main control variable for control of tubular reactors (which are similar to plate reactors for control purposes) has been the cooling flow rate or inlet temperature of the cooling water, see for example [Smets *et al.*, 2002], [Karafyllis and Daoutidis, 2002] and [Shang *et al.*, 2002]. In some papers, like [Smets *et al.*, 2002], several different cooling temperatures are used along the reactor.

A common assumption of the papers mentioned above, is that there is only one reactant injection site, in the beginning of the reactor. In the OPR, to increase flexibility, multiple injection sites are possible. This is specifically important for reaction schemes with several consecutive

reactions, then the reactants can be injected after each other along the reactor flow path. This feature has many advantages, for example allows the OPR to be better utilized. Normally the amount of reactant possible to inject is limited by the cooling capacity around the injection site, in the OPR the reactant injections can be distributed to use the full cooling capacity.

Standard procedure is to have off-line computation of the constant amount of reactant that should be injected. However, due to errors in the feed concentration of the reactants or errors in the model used for process design, more energy than expected may be released in the reactor. Then it is vital to have some possibility to influence the temperature in the entire reactor. Remember that from Section 3.3, we saw that the impact from the cooling temperature/flow rate on the reactor temperature in the beginning of the reactor was small, due to the limited heat transfer area.

All this has lead us to believe that using a single control variable, such as cooling temperature or flow rate is not enough, especially when there are multiple reactant injection sites. We should therefore see what input variables that can be used to have accurate temperature control in the entire reactor.

Cooling temperature and flow rate

For accurate temperature control of the reactor, it seems that manipulating the cooling temperature gives better control authority than the cooling flow rate.

First we consider the case when manipulating the cooling flow rate and the inlet temperature is constant. From Figure 3.5, it is clear that the gain from a change in cooling flow rate to cooling temperature saturates for large flow rates. There is also a nonlinear relation between the heat transfer coefficient and the cooling flow rate that may add to the model uncertainties, if it is used for control purposes.

Then we consider manipulating the cooling temperature with a constant flow rate. Figure 3.4 shows that the slope of the cooling temperature profile is fixed, but the offset of the slope changes. By manipulating the cooling temperature instead of the flow rate, we can better control the temperature difference and therefore the amount of heat transfer from the reactor. Therefore, in an emergency it is also better to change the cooling temperature than just the flow rate. A disadvantage of using the temperature as control variable instead of the flow rate is the higher complexity of the flow equipment.

However, it should be noted that the cooling temperature/flow rate have both limited impact on the temperature in the very first part of the reactor due to the limited heat transfer area. Dynamical analysis of the OPR shows that the temperature in the very beginning of the reactor is mainly determined by the reactant feed concentrations and temperature. Another disadvantage is the heat transfer dynamics between the cooling side and the reactor side, that introduce limitations on how fast and how well the reactor temperature profile can be controlled.

Feed concentrations and flow rate through reactor

Typical control variables used in many process control books are the feed concentrations of the reactants or the flow rates of the reactants. A drawback with the former variables is that it may disrupt the stoichiometric relations between the reactants A and B, since it is very difficult to verify that the desired feed concentration is really achieved without reliable concentrations measurements. To control the OPR by varying the total flow rate, will effect the hydraulic, thermodynamic and micro-mixing properties of the reactor. In addition the reactant flow through the reactor mainly affects the productivity and is less important for the chemical conversion. Thus the feed concentration and feed flow rate will be held constant during operation, to values determined during the initial process design phase.

Feed temperatures of the reactants

The inlet temperatures of the reactants can be used to control the temperature in the first part of the reactor, see Figure 3.6. With two small heat exchangers mounted at the inlet feed pipes to the OPR, the inlet temperatures can be manipulated. The residence time from the inlet to the outlet of one OPR plate is roughly 30 seconds. This will give a large time delay if the outlet reactant conversion is to be controlled by any of the inlet variables mentioned in this section. The effect of a change in the inlet temperature is also decreasing along the reactor length as the influence of the cooling flow increases for the later part of the reactor. However, if the reaction is difficult to ignite, it might be useful to be able to manipulate the feed temperature.

Distribution of the injected reactant B among the injection sites

When the process has multiple injection sites, the amount of reactant injected in each site is often calculated off-line and then held constant. To increase flexibility of the control system, we suggest that the distribution of the reactant injections is considered for control purposes. The total injected flow of reactant B remains constant during operation, so that the stoichiometric relation is fulfilled at least in steady-state. By varying the fraction of the total injection flow of reactant B, the heat released from the reaction can also be distributed. This means that by redistributing the injection flows, the released heat can also be redistributed. In combination with the control of the inlet temperature of the cooling water, we can achieve improved control of the reactor temperature.

The control signals

Based on the evaluations above, the following input variables are chosen as control signals.

- The first control variable is the injection flow of reactant B; more specifically, this variable determines how the reactant is distributed among the different injection points along the reactor. To guarantee stoichiometric balance the total flow rate of reactant B is fixed and the control signal u_1 denotes the fraction injected at the first point. The remainder, $(1-u_1)$ is injected at the second point. The total flow rate of reactant B is thus constant at all times.

- The second control variable is the inlet temperature of the cooling water u_2. The cooling temperature affects the total heat exchange, but has a limited impact on the temperature in the beginning of the reactor. The flow rate of cooling water is constant and determined so as to ensure good flow conditions for the heat transfer.

Note that u_1 controls where the energy is released inside the reactor, whereas u_2 can control the total amount of energy being transferred from the reactor. It is therefore essential to use both control signals to arbitrarily control the two temperature maxima and operate the OPR in a efficient and safe manner.

Besides u_1 and u_2, there can be additional control variables to further enhance flexibility. To improve conditions for start-up control, the feed temperature of the reactants can be added as a control variable. In the case when there are several independent cooling/heating zones, their different inlet temperatures can be added as control variables. To increase flexibility in the reactant injections, the total flow rate of B may also be varying.

Linear analysis of the OPR

To quantify the OPR dynamics, a linear analysis with Bode diagrams is made. The output variables are the two maximum temperatures, one after each injection point. The control variables were presented above. A linear model of the OPR can be written as the following transfer function matrix:

$$\begin{bmatrix} y_1 \\ y_2 \end{bmatrix} = \begin{bmatrix} G_{11} & G_{12} \\ G_{21} & G_{22} \end{bmatrix} \begin{bmatrix} u_1 \\ u_2 \end{bmatrix} \tag{3.3}$$

Linearization around a working point gives the steady state gains:

$$\begin{bmatrix} G_{11}(0) & G_{12}(0) \\ G_{21}(0) & G_{22}(0) \end{bmatrix} = \begin{bmatrix} 179.2 & 0.2 \\ -283.2 & 2.9 \end{bmatrix} \tag{3.4}$$

The difference between the gain from u_1, the reactant distribution, to the maximum temperatures and the gain from u_2, the cooling temperature, can be explained by different scalings of the control signals, $u_1 \in [0,1]$ and $u_2 \in [10,90]^\circ$ C. The fact that the reaction rate depends exponentially on the temperature also adds to the difference. A unit step change in reactant injection distribution corresponds therefore to a total shift of injections from one site to another, whereas a unit step change of the cooling temperature has a much smaller impact on the process.

It can also be noted that $G_{12}(0) \ll G_{22}(0)$, that is, the gain from cooling temperature to the first temperature maximum is much smaller than the one to the second maximum. It comes from the very limited heat transfer area around the first temperature maximum. This is in line with the steady-state simulations in Figure 3.4.

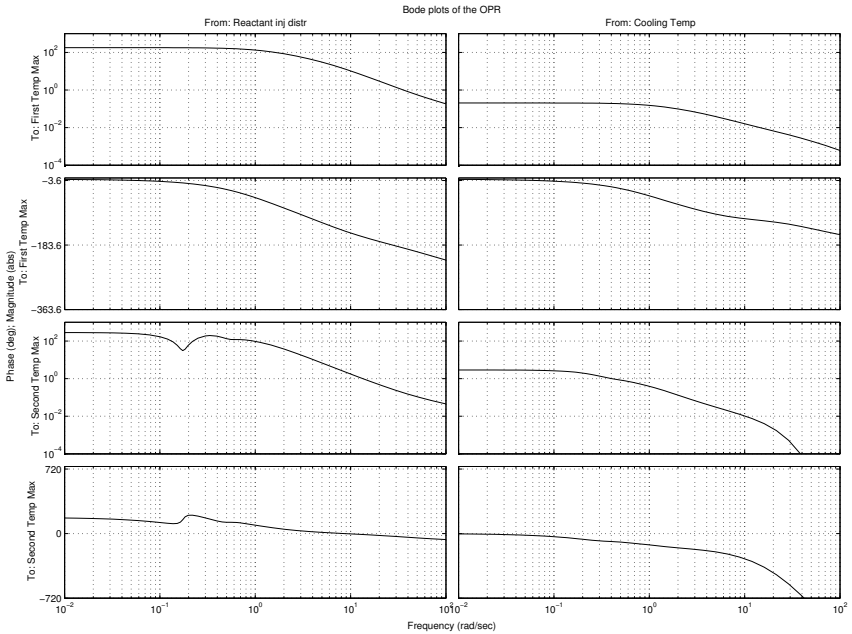

Figure 3.11 Bode diagram of the OPR with reactant injection distribution (u_1), left column, and cooling temperature (u_2), right colum, as control signals. The two output variables are the first temperature maximum and the second temperature maximum, upper row and lower row respectively. See also the Eq. (3.3).

Bode diagrams of the linearized process with the chosen control variables are shown in Figure 3.11 and 3.12, where the output variables are the two maximum temperatures and the two outlet concentrations of the reactants, respectively. In Figure 3.12, we can see that the transfer functions from u_1 to the two outlet concentrations are the same as well as from u_2 to the concentrations, since the two reactants are stoichiometrically related.

The steady state gains in Eq. 3.4 and the Bode diagram in Figures 3.11, show that the OPR has a lower-triangular structure. The cooling temperature mainly effects the second temperature maximum, whereas the reactant distribution affects both maxima. This implies

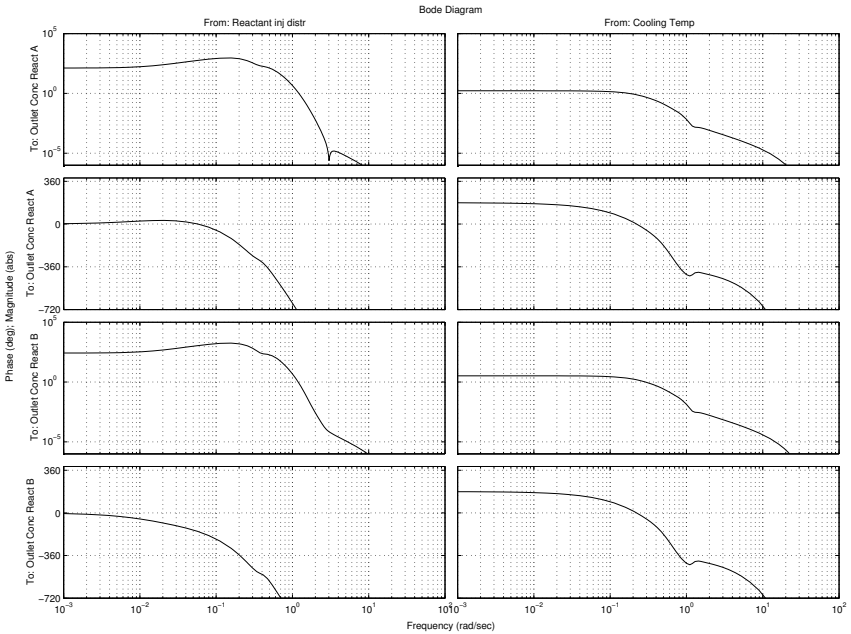

Figure 3.12 Bode diagram of the OPR with reactant injection distribution (u_1) and cooling temperature (u_2) as control signals. The two output variables are the outlet concentrations of the reactants A and B.

that with this choice of control variables, the cross-coupling effects between each control variable is present, but not large. So control of the OPR with these control variables should be feasible and straightforward.

The rest of the 11 inlet variables in Figure 3.1 are assumed to be constant or are controlled to keep a constant value. The flow rate of reactant A and the total flow rate of B are both controlled by standard Proportional-Integral controllers. The inlet temperatures of the reactants A and B are not controlled, but the measurements can be fed forward to improve disturbance rejection. The inlet feed concentrations of A and B are assumed to be constant during production, but they cannot be measured and are therefore a main source of input disturbances.

4

Process control of the OPR

In the previous section, suitable control variables were chosen. In this chapter we will elaborate on the control objectives, a suitable control structure and control algorithms. The control system is then evaluated in simulations with the nonlinear model of the OPR. First we will give a short review of potential methods used for process control of continuous chemical reactors.

4.1 Related work

For control purposes, the OPR can be viewed as a continuous tubular reactor. There is a limited number of papers in the literature on the subject, but there is a wide range of different control methods used for the control design of tubular reactors.

In [Luyben, 2001] the focus is on plant-wide control using conventional selective control scheme. The effect of design and kinetic parameters on the controllability is also studied. To control the maximum temperature inside the reactor, several internal sensors are used and their data is sent to a selector, which singles out the maximum temperature for feedback to a PI-controller. The main advantage is the simplicity of the feedback controller, however it is not always trivial to find a suitable reference temperature for the reactor that gives optimal conversion.

In [Karafyllis and Daoutidis, 2002] a nonlinear control law based on feedback linearization for a distributed parameter system is derived.

The aim is to have the maximum temperature inside the reactor follow a desired reference temperature. The manipulating variable is the cooling temperature. The result is verified for both model and measurement errors. Also here, the choice of reference temperature is not discussed.

In [Smets *et al.*, 2002] optimal control theory is used to derive open-loop analytical solutions for the cooling temperature to maximize the performance. The performance criterion is defined as a combination of minimizing the outlet concentrations of the reactants and the global heat loss. One of the interesting results is the nearly optimal solution where a bang-bang cooling temperature profile is used. One cooling temperature is used for the first part of the reactor and after some switching point, another cooling temperature is used. This fits very well into the OPR framework, where the flexible configuration allows several different cooling flows to be used. However, limitations on the maximum reactor temperature are not considered and the open-loop control solution is sensitive to model uncertainties and process disturbances. The work has also been extended to tubular reactors with various degrees of dispersion, see [Logist *et al.*, 2005a; Logist *et al.*, 2005b].

In [Hudon *et al.*, 2005] adaptive extremum seeking control is applied to a non-isothermal tubular reactor with unknown kinetics with interesting results. The main contribution is to allow for optimal control even in the presence of uncertainties, when the actual optimal operating point is unknown. The paper assumes there are a finite number of control actuators to implement the calculated optimal cooling profile.

In [Shang *et al.*, 2002] characteristics-based Model Predictive Control is used to control the outlet concentration in a plug-flow reactor by manipulating the cooling flow rate. The main focus is on the significant computational benefits with the characteristics-based MPC compared to finite difference based MPC. However, since an endothermic reaction is studied, the issue of hot spots and temperature constraints are not discussed in that paper. Other characteristics-based feedback control methods are described in [Shang *et al.*, 2005].

In the references above, the reactant B is only injected in the beginning of the reactor, and consequently the performance and safety of the reactor is controlled using only a single variable, in general the cooling temperature or flow rate. When there are multiple injections,

the control methods need to be extended.

In [Luyben, 2001] and [Karafyllis and Daoutidis, 2002] the control objective is limited to control the maximum temperature inside the reactor. The main advantage is the simplicity, since no concentration estimates are needed. It is then assumed that as long as the temperatures inside the reactor is controlled, the concentrations and chemical conversion will be good. However, neglecting the concentrations in the control design, may lead to suboptimal conversion due to model errors.

For the control of the OPR, the optimal cooling temperature profiles from [Smets *et al.*, 2002], the adaptive scheme of [Hudon *et al.*, 2005] to handle unknown kinetics and the optimization and computational efficiency in [Shang *et al.*, 2002] are of most interest.

4.2 Interesting control challenges of the OPR

In this section we will briefly summarize what problems, the control system for the OPR will have to deal with.

As described in Chapter 2, the process is highly nonlinear with the reaction rate being an exponential function of the temperature. The exothermic character of the reaction leads to heat release and may lead to instability, a so called runaway reaction. It is therefore a main priority for the control system to ensure safe operation of the OPR, for example by using temperature constraints that should not be violated.

The OPR is designed for a steady state optimal operating point, but optimality has to be preserved even during production when there are uncertainties or process disturbances. It is then essential that the control system can adjust the input variables to maintain a high level of performance, in this case chemical conversion. The feedback control based on internal measurements will facilitate this adjustment and can compensate for inexact pumps and valves or variations in the feed quality. It reduces the time to obtain desired performance compared to manual trial-and-error adjustments of the input variables.

The control system also has to deal with output feedback, since only temperature measurements are available. Estimation of concentrations will be necessary to improve robustness to these disturbances.

4.3 Control objectives and control methods

Control objectives

The control objective for the OPR can be stated as an optimization of the reactant conversion γ, see Eq. (3.1) with constraints on both control and state variables, such as temperatures. As mentioned before, it is critical that the temperature inside the reactor can be controlled to stay below some safety limit. The optimization can be expressed as:

$$\max_{u \in \mathcal{U}} \gamma(x,u,d) = \frac{c_C}{c_C + c_A} \quad \text{so that} \quad Wx \leq \Omega \tag{4.1}$$

where x are the state variables; temperatures and concentrations along the reactor. u are the two control signals, $\mathcal{U}$ is the admissible control set, d are exogenous disturbances and W and Ω define the state constraints. Note that γ is a nonlinear function of the concentrations and they in turn depend on the reactor temperature.

Control methods

We know from Section 3.3 that an increase in reactor temperature improves the conversion. So for this specific reaction, the optimal operating point will be on the temperature safety constraints. The closer we can operate the process to the constraints, the better performance and productivity is achieved. This implies that it is necessary to choose a control algorithm that combines optimization and constraint handling. This type of control problem is well suited for Model Predictive Control (MPC), see [Qin and Badgwell, 2003] or [Maciejowski, 2002], due to its ability to handle explicit input and output constraints and optimization of a cost function.

Another alternative is to use PID-controllers with selectors, similar to [Luyben, 2001], to control the maximum reactor temperature to some reference value. The lower triangular structure of the process, from Eq. 3.4 and Figure 3.11, originates from the fact that the reactant distribution affects the two temperature maxima, whereas the cooling temperature mainly affects the second maximum. The cross-couplings between the control signals are weak, which may allow for PID-control without a decoupling matrix. For this exothermic reaction, there is a

simple relationship between higher temperature and higher conversion, which is not true in the general case with competing reactions. Therefore it is straight forward to determine a temperature reference value that will lead to good performance. For other reactions, it may be non-trivial to determine the optimal temperature references. It is also necessary to leave some safety margin to the constraints. To prevent too high temperatures, gain scheduling can be used based on the measured maximum temperature, so the controller gain is increased for temperatures closer to the constraints.

However, in the end MPC was chosen for its ability of handling constraints and optimization framework.

4.4 Control structure

The two control variables chosen for process control are the reactant injection distribution u_1 of the two injection flows and the cooling temperature u_2.

These are achieved by manipulating one or more control valves on the flows leading into the reactor. Instead of applying the output of the MPC to the actual control valves, it can be advantageous to use MPC as a reference governor, see Figure 4.1. The MPC serves as a set-point generator to linear feedback loops that executes the low level control. The main advantages are that the nonlinear actuators are linearized and it enables manual control of the OPR input properties.

The process control system can also be viewed as cascade control structure, see Figure 4.2. The reference values $u_{1,ref}$ and $u_{2,ref}$ are sent from the MPC to two local feedback controllers. C_1 controls the reaction injection distribution with signals to the two injection valves w_1 and w_2. P_1 represents the flow and valve dynamics of the injections, see Section 4.5. C_2 controls the cooling inlet temperature with two control valves v_1 and v_2. P_2 represents the thermo-hydraulic system, where the cooling water is mixed to the desired temperature for the given flow, see Section 4.6.

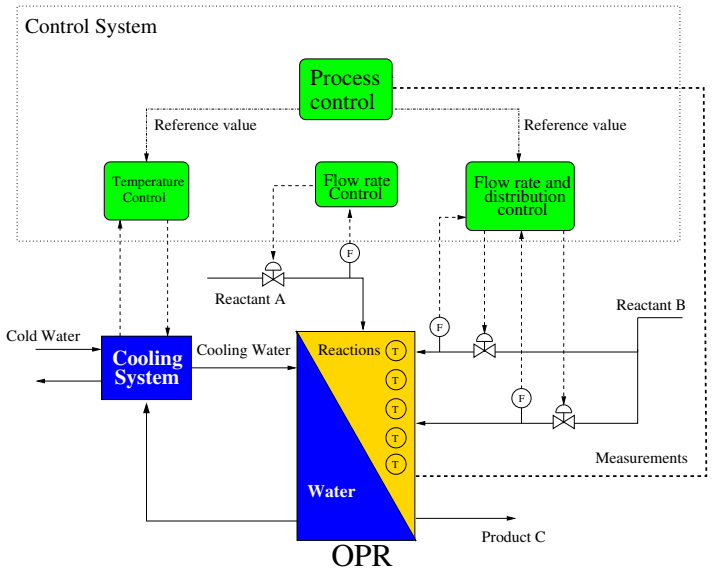

Figure 4.1 Schematic flow scheme for the OPR and cooling system together with the control system.

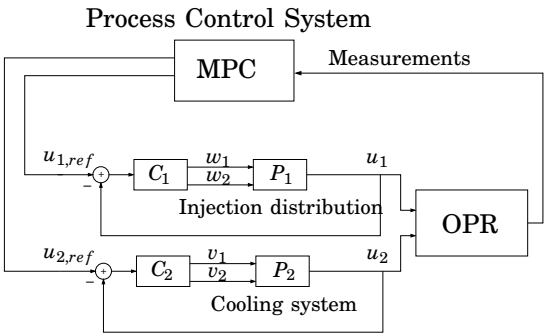

Figure 4.2 Control structure for the OPR. The process control system uses Model Predictive Control to calculate the optimal control signals u_1 and u_2. These signals are then sent to the injection distribution C_1 and cooling temperature C_2 controllers. P_1 and P_2 represent the process dynamics of the injection valves and the cooling system.

4.5 Reactant injection distribution control

The injection flow of reactant B should be distributed along the OPR as given by the reference signal from the MPC controller. Using standard ratio control, see for example [Shinskey, 1996] or [Hägglund, 2001], the desired distribution of the reactant B is achieved. A small control valve is mounted on each injection pipe. The first injection flow rate is controlled to $u_1 \cdot q_B$ and the second injection flow rate is then controlled to $(1-u_1)\cdot q_B$, ensuring constant total injected flow rate q_B at all times.

However due to the spatial difference in injection sites from the inlet to the middle of the reactor, the flow time constitutes a delay of around 15 seconds between injection sites. The injection flow controller does not take the flow time into specific consideration. This means that a change in $u_{1,ref}$ will cause a short transient in stoichiometry, before perfect balance is once again achieved. However it is important to note that the transient time can be neglected compared to a planned production time of 24 hours a day. To increase control flexibility it could also be possible to have independent control of the two injection flow rates instead of using ratio control. Then a soft constraint is added to guarantee that the correct total flow rate is achieved in steady-state.

4.6 Utility system

A utility system and a temperature controller have been designed and experimentally tested, to have accurate control of the inlet temperature of the cooling water. In this section the utility system is briefly presented, a more detailed description of the utility system, its controller and the performed experiments can be seen in Chapter 5.1

The flow configuration shown in Figure 4.3 is a standard flow circuit for heating or cooling purposes, see [Petitjean, 1994]. With recycle of the water coming out from the OPR directly back to the control valve RV1, the speed of the temperature control can be significantly improved. The second recycle, around the heat exchanger HEX to the left, is implemented to keep the flow rate through the heat exchanger, $FT2$, constant regardless of the valve position of RV1.

The cooling inlet temperature $TT5$ should follow a given reference temperature. The cooling flow rate $FT3$ is generally kept constant.

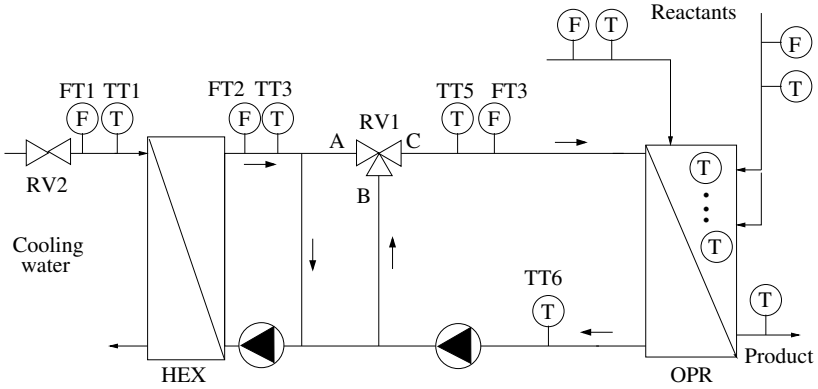

Figure 4.3 Flow configuration of the cooling system with recycle loops around the heat exchanger (HEX) and the OPR. Note that the control signals v_1 and v_2 corresponds to the positions of control valves RV1 and RV2. The output signal u_2 in Figure 4.2 refers to the cooling inlet temperature TT5.

The main control signal v_1 is the position of control valve RV1. The second control signal v_2 is the position of control valve RV2, which indirectly controls the outlet temperature $TT3$. By combining the two control signals in a mid-ranging control structure, see Figure 4.4, we can control the cooling inlet temperature $TT5$ and also keep the control valve RV1 close to some desirable working point, for example 50%, to avoid valve saturation. The input-output dynamics of the utility system and its controller in closed loop have a time constant of roughly 5 seconds.

4.7 Model predictive control of the OPR

In this section, an MPC controller will be designed to control the OPR in the nominal control mode (see Section 3.4), that is, during nominal operation after the start-up transient. The main objective is to ensure safe production and maximize the conversion with constraints on input and state variables.

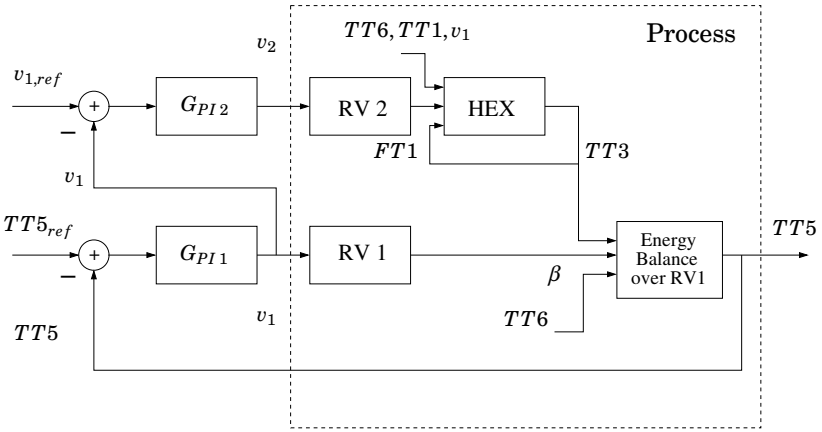

Figure 4.4 Mid-ranging control structure of the utility system. PI-controller G_{PI1} controls the cooling inlet temperature $TT5$ and G_{PI2} acts such that v_1 works around a desirable working point specified by $v_{1,ref}$. The dashed square denotes the cooling system process, compare with the control structure in Figure 4.2. Note that $TT5_{ref}$ and $TT5$ correspond to $u_{2,ref}$ and u_2 in Figure 4.2, but $v_{1,ref}$ is a constant and not included in that figure.

The reaction used in the simulations is as stated earlier oxidation of thiosulfate by hydrogen peroxide, a fast and exothermic single liquid-phase reaction.

$$2Na_2S_2O_3 + 4H_2O_2 \rightarrow Na_2S_3O_6 + Na_2SO_4 + 4H_2O \qquad (4.2)$$

The kinetic reaction parameters are $k^0 = 2 \cdot 10^{10}$ L/(mol s), $E_a = 68200$ J/mol and $\Delta H = -586000$ J/mol thiosulfate, for use in Eq. 2.7.

The model

A nonlinear model of the OPR and the reaction kinetics was derived from first principles, in Chapter 2, and a linear MPC controller is developed based on notations from [Maciejowski, 2002] and [Åkesson, 2003]. The nonlinear model is linearized around some operating point (x^0, u^0), which is assumed to be close to the optimal point. The linear system

is sampled with $h = 1.0$ seconds to a discrete-time system. Based on the dynamic analysis and the estimated time constants in Section 3.3 in combination with rules of thumb from [Åström and Wittenmark, 1997], h should be less than 0.5 seconds. On the other hand, the time constant of the controlled cooling system is roughly 5 seconds, so there is little use of using $h < 0.5$ s, since the cooling temperature cannot be actuated that fast. Also, shorter sample time requires longer prediction horizon, which increases the computational effort of the MPC, see the discussion below. And finally, the residence time of the OPR is roughly 30 seconds. In total, the choice of $h = 1.0$ s seems adequate.

$$x(k+1) = Ax(k) + B_1u_1(k) + B_2u_2(k) + B_dd(k) \tag{4.3}$$

$$y = C_yx(k) \tag{4.4}$$

$$z = C_zx(k) \tag{4.5}$$

The OPR is approximated as a long tubular reactor and is discretized in n equal elements. To simplify the model and keep the number of states low, fewer discretized elements were used to model the OPR for control design compared to the open-loop simulations in Chapter 3. There are five states in each element, the temperature in the reactor and in the cooling water and the concentrations of the two reactants and one of the products, see Eq. (4.2) for the chemical composition. That gives the linear model $5n$ states. The control design in the thesis is based on $n = 10$.

Control design and cost function

The two control signals are reactant injection distribution u_1 and cooling temperature u_2. There are seven possible inlet disturbances d, see Figure 3.1, however, all but the feed concentrations can be measured and compensated for by feed forward. The available state measurements y are 10 temperatures inside the reactor, the sensors are assumed to be placed equally spaced along the reactor. The inlet and outlet temperatures of the cooling water are also measured, in total 12 signals.

The conversion γ that we want to maximize was defined in Chapter 3 as

$$\gamma = \frac{c_C}{c_C + c_A} = \frac{c_{product}}{c_{product} + c_{reactant}} = \frac{c_{Na_2S_3O_6}}{c_{Na_2S_3O_6} + \frac{1}{2}c_{Na_2S_2O_3}} \tag{4.6}$$

where the factor $1/2$ is the inverse of the stoichiometric coefficient from Eq. (4.2). γ is a nonlinear function of the state variables, so it has to be rewritten before it can be used in the cost function of the MPC theory. Remember that we assume constant feed flow rates of reactant A and B, but the distribution of reactant B is one of the control variables.

The first alternative is to maximize the outlet concentration of product C. One issue here is what reference to use in the cost function Eq. (4.7). A natural choice would be the outlet concentration corresponding to 100% conversion, however if the feed concentrations are higher than expected, this choice would lead to tracking of a suboptimal reference value.

Another alternative is to minimize the outlet concentrations of the two reactants in the cost function. As long as the feed flow rates of the reactants are constant, this would also lead to a maximum of the conversion. Here the choice of a reference value is easy to choose, since zero corresponds to complete conversion regardless of any changes in the feed concentrations.

The controlled variables z are therefore chosen to be the outlet concentrations of the two reactants. The cost function to be minimized is

$$V(k) = \sum_{i=1}^{H_p} \|\hat{z}(k+i|k) - r(k+i|k)\|_Q^2 + \sum_{i=0}^{H_u-1} \|\Delta\hat{u}(k+i|k)\|_R^2 \tag{4.7}$$

The constant reference signals are set to $r = [0 \quad 0]^T$, corresponding to all reactants being consumed and $\gamma = 100\%$.

Regardless of variable used in the cost function, the feasible cost function will not be symmetric around the minimum, since physical limitations confine the process to right hand side of the cost function, see Figure 4.5, thus emphasizing its linear term.

Constraints

There are constraints on the temperatures inside the reactor due to safety concerns, for example boiling or undesired by-product formation. During the process design, a safety analysis should be made and a maximum temperature determined at which it is safe to operate, but temperatures above it should be avoided. In this thesis $T_i \leq T_{max} =$

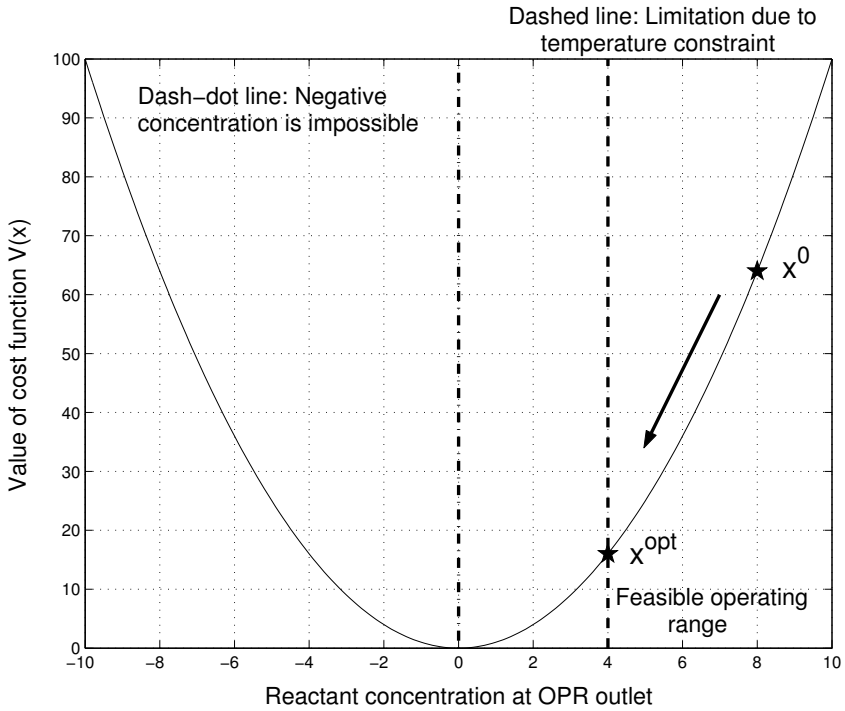

Figure 4.5 Schematic figure of the cost function for a chemical process. The objective is to find a control sequence that brings the process from starting point x^0 to the minimum $V = 0$. However, the temperature constraint (dashed) limits how close to optimum we can get, x^{opt}. The dash-dot line indicates that negative concentration is impossible.

$90°C$, where T_i is the temperature in the i:th element of the model and $1 \leq i \leq 10$.

There are also constraints on the control signals; the reactant injection distribution is restricted to $0.1 \leq u_1 \leq 0.9$, that is, not all reactant B can be injected in the same point, due to micro-mixing limitations. The cooling temperature is limited to $10°\text{C} \leq u_2$. The lower limit is set by the temperature of the main water system of the plant or a nearby river or lake. Due to the recirculation of the cooling water, there is no

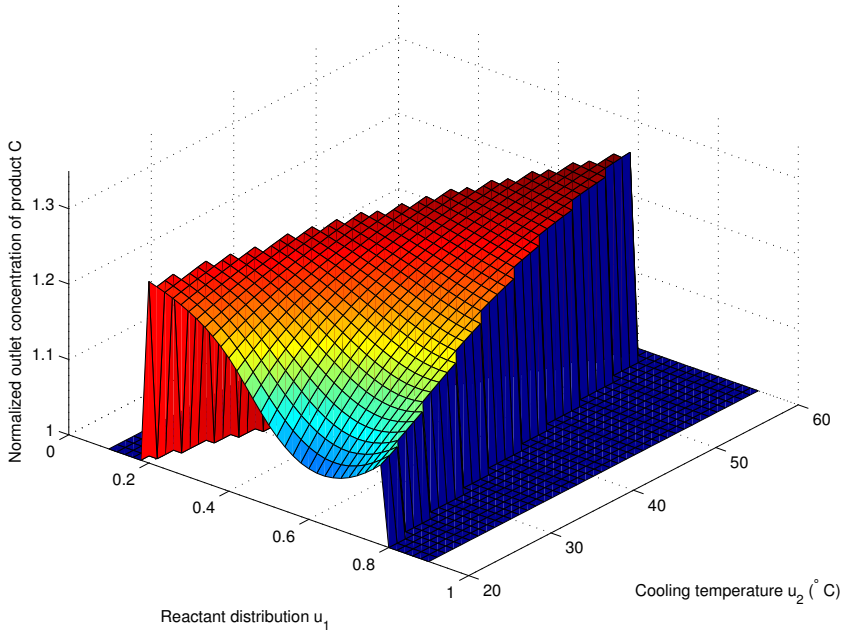

Figure 4.6 The outlet concentration of the product C for varying values of the control variables. Only the results from feasible input signals are plotted, which in steady state give reactor temperatures below the constraint level.

constraint on the upper cooling temperature. The change in the control signals are limited to $|\Delta u_1| \leq 0.2$ per second and $|\Delta u_2| \leq 1°\text{C/second}$.

The input constraints are hard constraints, whereas the state constraints are soft. However, since the reactor temperature should not be above the safety limit, the penalty on the ∞-norm of the slack variables ϵ should be chosen very large, see [Maciejowski, 2002], to recover the same solution as if the state constraints were hard.

Feasible regions

In Figure 4.6, the normalized outlet concentration of the product C is plotted for varying values of the two control variables. The figure

will help us understand the relations between inputs and outputs in combination with the introduced constraints. If the control variables are such that they cause reactor temperatures above $T_{max} = 90°C$, the concentration value is set to 1.0. It is then easy to identify the feasible ranges of the control variables. The nonlinear relation between temperature and outlet concentration is clearly visible. There is a unique concentration maximum of 1.275 for $u_1 = 0.62$ and $u_2 = 58°C$ in the right corner of the feasible region. It is the optimal point in line with the process design, where the two temperature maxima are both at 90°C.

However, for the left corner, where $[u_1\, u_2] = [0.18\, 20]$, the outlet concentration is almost as high; 1.241. In this case, almost all of reactant B is injected in the midsection and to keep the temperature maximum at 90°C, the reactor is cooled with the lowest cooling temperature available. The high outlet concentration can be contributed to the high concentration that follows from 82% of reactant B being injected in the same spot. This is not a desired operating point, since the reactor is not utilized in a reasonable manner. To improve productivity in both cases, higher feed concentrations should be used.

There are further implications from Figure 4.6. The process design resulting in that graph may affect the control design. If the control system relies on an MPC optimization of the outlet concentration with a short prediction horizon, it is easy to see that there is a large probability that the system will end up in the "wrong" corner, the left one where $[u_1\, u_2] = [0.18\, 20]$. For some choice of weight matrices, prediction and control horizons, the controller will not "see" the advantage of the more balanced injection scheme $[u_1\, u_2] = [0.62\, 58]$.

For another choice of process design, the implications on the control system will be different. For example, if the feed concentration is increased with 20% to better utilize the OPR, another set of feasible region is calculated, see Figure 4.7. Since more heat is released from the reaction, the feasible region of the control variables is significantly smaller. Again there is an unique maximum in product concentration of 1.526 in the right corner of the region, whereas the suboptimal left corner yields a concentration of 1.503.

The main message from the two figures above is that the process design has serious implications on the control design and they should not be seen as separate stages during the design phase.

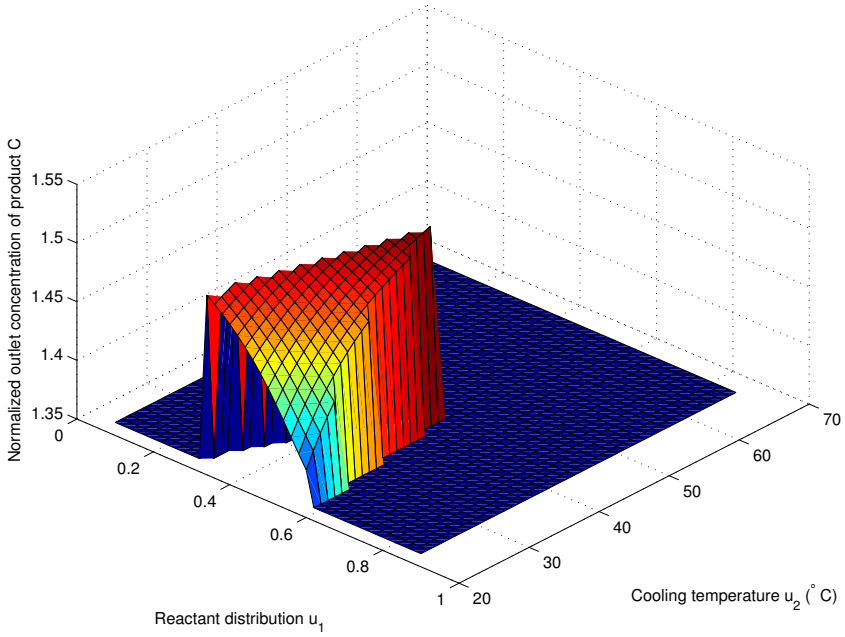

Figure 4.7 The outlet concentration of the product C for varying values of the control variables when feed concentrations are increased by 20%. More heat is released, thus decreasing the feasible region of the input variables. Only the results from feasible input signals are plotted, which in steady state give reactor temperatures below the constraint level.

Tuning parameters

The prediction horizon is chosen as $H_p = 160$ and the control horizon $H_u = 8$. For a complex process like the OPR, it is necessary to choose a reasonably large prediction horizon H_p, such that all important process dynamics can be observed within the prediction window and the online optimization will "see" the best operating point in the feasible region, see the discussion in previous section. In this case the prediction time is $H_p \cdot h = 160$ seconds, to be able to cover the thermal dynamics, the residence time and to increase the stability of the system. To reduce

the computational complexity it is possible to have a longer sampling interval h, which allows for a lower value of H_p. However for good disturbance rejection property a short sampling interval is desired.

The weighting matrices for the controlled variables and the control signals are chosen as $Q = 10^{-5} \cdot \mathbf{I}$ and $R = [1000 \quad 0; 0 \quad 1]$. The difference in weights on the control signals is partially due to a difference in the units of u_1 and u_2. It is also desirable to favor the use of the cooling temperature over the injection distribution, since the latter causes a temporary change in the stoichiometric balance. The weight Q on the controlled variables is very low, since the main priority is to stay below the safety constraints and the output weight mainly determines how long it will take before the process reaches the temperature constraints.

With the current choice of weight matrices Q and R, the closed-loop dynamics of the OPR and the MPC are slow compared to the closed-loop dynamics of the injection distribution and cooling system. It is therefore possible to neglect the closed-loop dynamics of the these two subsystems in the MPC control design. In the simulations, however, the cooling system is modelled by Eq. (5.5) using the same control structure and control parameters as in the experiments. The injection distribution dynamics are very fast and can therefore be neglected also in the simulations. If the closed-loop dynamics of the OPR are desired to be faster, the cooling system dynamics should also be included during the MPC control design.

State and disturbance estimation

In MPC, full state feedback is used and since the concentrations are not possible to measure, state estimation is required. In addition, there are process disturbances and measurement noises that need to be considered. The primary input disturbances are the feed concentrations. There can also be varying inlet temperatures of the feed reactants, but they can be measured and compensated for with feed forward.

The state vector x is therefore augmented with two constant disturbance states x_d, corresponding to unknown feed concentrations. The estimates of the disturbance states will be used by the MPC algorithm and may lead to disturbance rejection. It is also possible to include extra disturbance states to allow for estimation of unknown model parameters, such as the kinetic activation energy E_a.

For the augmented system, an extended Kalman filter (EKF) is designed based on [Dochain, 2003], which provides state, disturbance and parameter estimations to the MPC controller. The EKF uses the full nonlinear model of the process and calculates the covariance matrix $P(\hat{x})$ as the solution of the dynamical Riccati matrix equation, which minimizes the variance of the estimation error, see Eq. (4.8)-(4.10). R_1 and R_2 are the variances of the process and measurement noise, respectively. The nonlinear model is linearized symbolically. The state matrix $A(\hat{x})$ is then evaluated in each sample with the current state estimates $\hat{x}$.

$$\frac{\mathrm{d}\hat{x}}{\mathrm{d}t} = f(\hat{x}, u, d) + K(\hat{x})(y - \hat{y}) \tag{4.8}$$

$$K(\hat{x}) = P(\hat{x}) C_y^T R_2^{-1} \tag{4.9}$$

$$\frac{\mathrm{d}P}{\mathrm{d}t} = -PC_y^T R_2^{-1} C_y P + PA^T(\hat{x}) + A(\hat{x})P + R_1 \tag{4.10}$$

The estimations of cooling temperatures are regarded as more certain than the reactor temperatures. They are in turn more certain than the reactor concentrations and to emphasize estimation of the feed concentrations, they are regarded as most uncertain. This can be represented by the variance matrices

$$R_1 = \mathrm{diag}([1...1\ 0.001...0.001\ 100...100\ 1000\ 1000]) \tag{4.11}$$

$$R_2 = \mathrm{diag}([1...1]) \tag{4.12}$$

where the entries of R_1 are in the following order; n reactor temperatures with variance 1, n cooling temperatures with variance 0.001, $3n$ reactor concentrations with variance 100 and finally two feed concentrations with variance 1000. The variance of the measurement noise R_2 can be adjusted to achieve the desired convergence rate of the estimation, but should also capture the variance of the real measurement noise of the twelve temperature sensors.

Discussion of the control design

To summarize, a linear MPC controller has been designed to control the nonlinear OPR process. An extended Kalman filter is used for non-

linear state and disturbance estimation. There are linear constraints on the reactor temperature to emphasize safe operation.

Integral action is a vital property of the closed loop system and methods have been derived to achieve this, see for example [Åkesson and Hagander, 2003] or [Pannocchia and Rawlings, 2003]. It is characterized as rejection of constant input or output disturbances, which is handled very well by the EKF, due to its nonlinear structure. The estimates of the disturbances are sent to the MPC, which compensates for them. Another property of the integral action is set-point tracking, which follows from the use of disturbance estimation. However, the MPC uses a linear process model, whereas the EKF uses a nonlinear model. This may give zero estimation errors, but it also means that the EKF does not include the model errors between the linear model used by the MPC and the nonlinear process, which may disrupt the guaranteed set-point tracking. The MPC will then get the correct state values $\hat{x}(k) = x(k)$, but in the optimization the linear prediction model leads to an erroneous control signal $\Delta u(k)$ being calculated.

However, tracking is usually never an important issue for the OPR, since in general physical limitations in the reactor temperature render set-point tracking of the concentration references infeasible, see Figure 4.5. In process control of the OPR it is therefore more important to have accurate state estimation to respect the temperature constraints, than to strive for set-point tracking.

When MPC is used for online control, the computational complexity is an important issue. The complexity increases with the number of constraints and states in the model, which largely depends on the number of discretization elements used in the prediction model. In [Shang *et al.*, 2002], the method of characteristics is used to achieve an accurate low-order model, which reduces the computational complexity. It is also significantly influenced by the choice of prediction and control horizons, which should be as long as possible from a stability and performance point of view.

We also have to note that with output feedback and a linear prediction model in the controller, there is a certain region of attraction for the closed loop system. To increase this region and to reduce model errors, nonlinear MPC can be used, which includes a nonlinear prediction model. The computations will then be more complex, but with more efficient software it may be feasible.

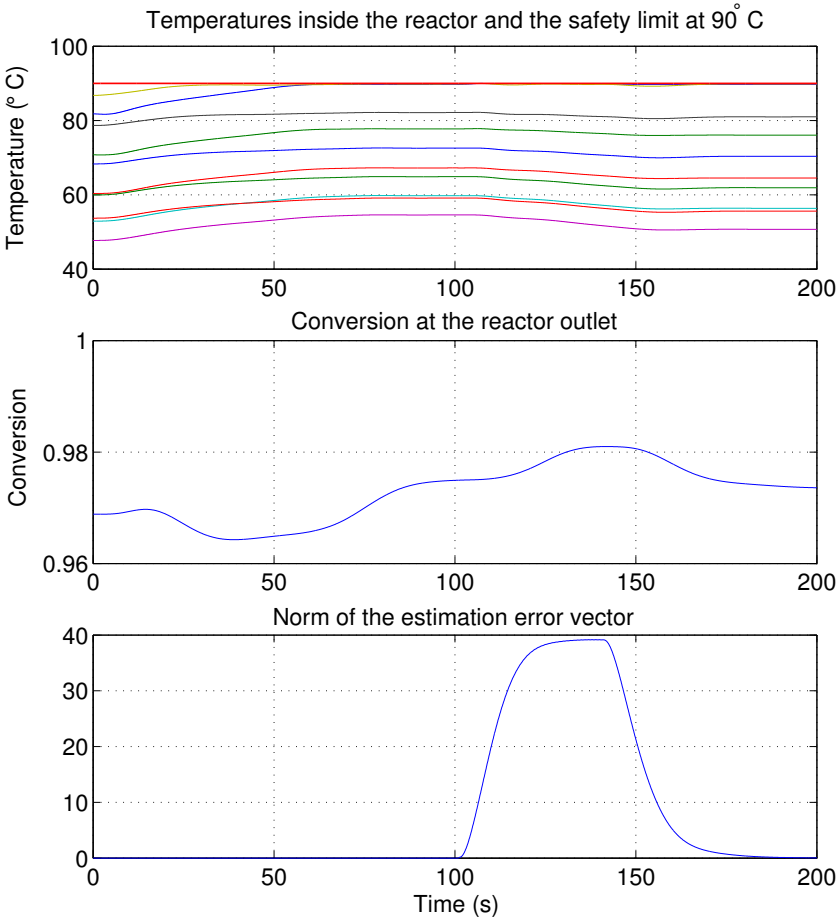

Figure 4.8 Upper plot: Temperature in the 10 elements of the reactor. Middle plot: Conversion at the reactor outlet. Lower plot: After the ramp disturbance in feed concentrations ends at $t = 140$ seconds, see also Figure 4.12, the norm of the estimation error vector quickly decreases.

4.8 Simulation results

In this section, the MPC and EKF design is evaluated in simulations with the nonlinear process model from Chapter 2. The MPC, EKF and the nonlinear model of the OPR are implemented in Matlab/Simulink using scripts from [Åkesson, 2003]. The reactor is discretized into $n = 10$ elements both for the nonlinear simulation model and the linear prediction model used by the MPC. The simulations can be divided into two parts. The first part, between $t = 0 - 100$ seconds, is the transient from a sub-optimal to an optimal operating point, where some temperature constraints are active. The second part, between $t = 100 - 200$ s, covers the case with a ramp disturbance in the reactant feed concentrations. Note that u_1 determines how large a fraction of reactant B should be injected at the first injection point. The remaining amount of reactant B $(1-u_1)$ is injected at the second injection point at the middle of the reactor.

Initial transient

The transients of the OPR are determined by the reference signals and the initial conditions. The reference values are set to $r = [0\,0]$ for the outlet concentrations of the two reactants A and B, which means that all reactants should have been consumed before they reach the end of the reactor. This implies that one or more temperature constraints may be active at steady-state, since full conversion may require temperatures above the allowed maximum. The process starts in steady-state in a non-optimal operating point and it is assumed that the observer states are correctly initialized.

To optimize the conversion, the MPC controller increases the temperatures inside the reactor by increasing the cooling temperature, see Figures 4.8 and 4.9 for simulation results. However, since the cooling temperature has a limited impact on the reactor temperature in the first part of the reactor, the reactant injection distribution was used to increase the temperature there. Figure 4.9, shows an increase in u_1 from 0.50 to 0.54, redistributing the reactant flow from the second to the first injection point. This corresponds to more heat being released from the reaction, thus increasing the temperature. The reactant redistribution causes temporary changes in the stoichiometric balance, resulting in a slight drop in conversion during the first 70 s, see mid-

plot in Figure 4.8. The flow time from the second injection point to the reactor outlet is around 15 s, which explains the time delay from the change in u_1 to the change in conversion. Meanwhile, the temperatures increase in the midsection of the reactor when the cooling temperature u_2 increases, despite less reactant being injected there.

After approximately $t = 50$ s, the temperatures around the two injection points have reached the safety constraint $T_{max} = 90$°C and by maintaining the temperatures just below the constraint level, the conversion continues to be as high as possible. Profiles of the temperature and the conversion along the reactor in steady-state at $t = 200$ s are shown in Figure 4.10. Note that the safety temperature constraint imposes the main limitation on reactor performance. As the cooling temperature of 37° C is well above the input constraint of $u_{2,min} = 10$° C, even higher reactant concentrations could have been used, thus increasing the productivity. Therefore also the lowest cooling temperature available can be seen as a process limitation.

The ramp disturbance

To test the disturbance rejection property of the EKF and the MPC controller, ramp disturbances in the feed concentrations of both reactants were introduced between $t = 100 - 140$ s, see Figure 4.12. The 5% increase in feed concentrations leads to larger amounts of reaction heat released inside the reactor, thus increasing the risk of violating the temperature safety constraints. Without disturbance estimation, the MPC fails to respect the constraints and the maximum temperature reaches 92°C in steady state, see Figure 4.11.

With the estimation, the MPC controller can ensure that the temperature constraints are only slightly violated during the ramp and afterwards in steady-state the temperatures stay on the constraint. The estimation is based on a constant disturbance model, which explains its inefficiency during the ramp.

During the disturbance, the MPC reacts by decreasing u_1 and u_2, that is, redistributing more reactant B to the second injection point and increasing the cooling of the reactor, see Figure 4.9. When the heat from the reaction is redistributed from the first to the second injection point, this will cause that temperature to increase even further. However, the MPC anticipates that effect and effectively increases the cooling to deal with both the disturbance and the redistribution

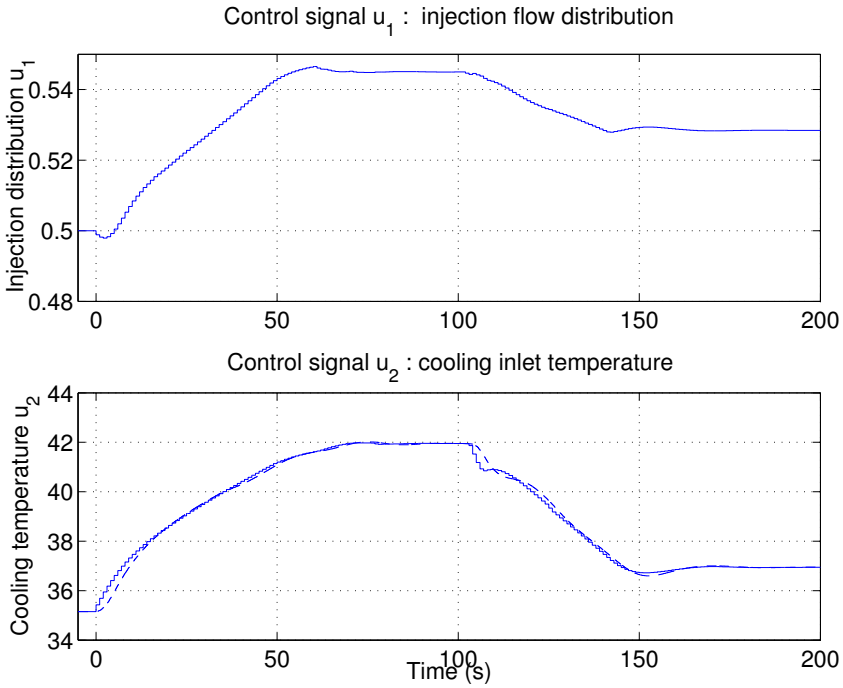

Figure 4.9 Control signals for the OPR. During the disturbance, u_1 redistributes reactant to the second injection site while u_2 decreases the cooling temperature. Together, these actions keep the reactor temperatures below the safety limit. In the lower plot the reference signal from the MPC is solid and the actual temperature of the water from the cooling system is dashed.

of reaction heat. This is a main advantage from using multivariable model-based control. The lower plot of Figure 4.8 shows the norm of the estimation error vector $e = x - \hat{x}$. When the ramp disturbances start at $t = 100$ seconds, the norm of the error increases to 40. After the inlet concentrations have reached their new steady-state values, the norm of the estimation error converges to zero within 40 s.

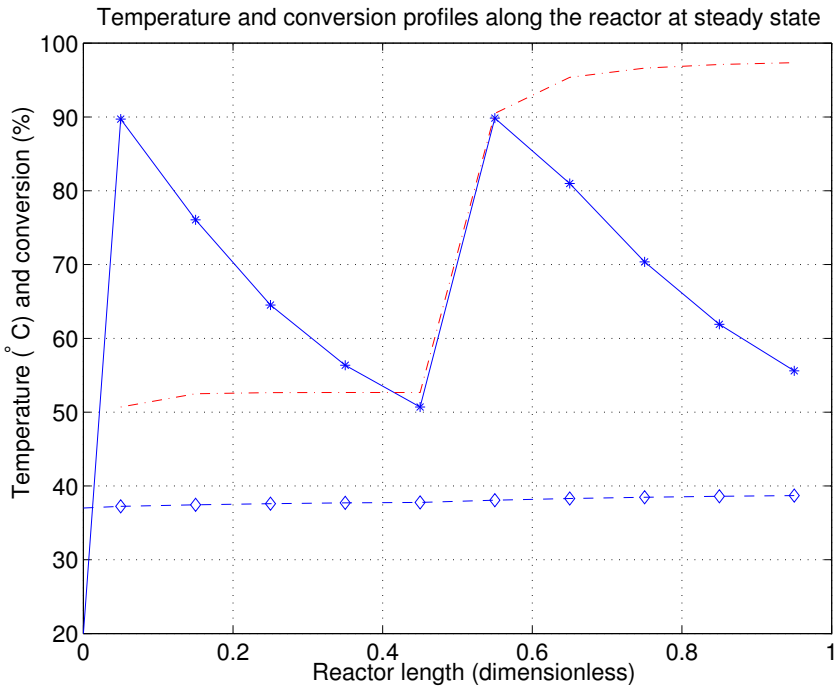

Figure 4.10 To optimize the use and performance of the reactor, the OPR is controlled such that the two temperature maxima are of equal height and just below the safety constraint. The reactor temperature (solid), cooling temperature (dashed) and conversion (dash-dot).

4.9 Summary of the control system

The simulations show that desired safety and performance of the OPR can be achieved with model predictive control, which combines explicit handling of constraints and optimization of the conversion. This allows for operation closer to the constraints, thus increasing the conversion. Secondly, for more complex reaction schemes, the optimization leads to reactor temperatures that maximize the conversion, based on the close relationship between temperature and concentration. The same efficiency can be achieved by manual calibration of the input variables,

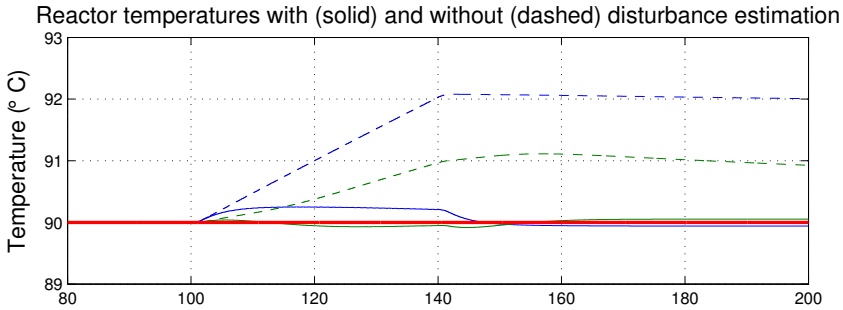

Figure 4.11 The two temperature maxima for the case with disturbance estimation (solid) and without (dashed).

however, that method is non-trivial and time-consuming.

The MPC serves as a reference signal generator to the two local subsystems that control the reactant distribution and cooling temperature, respectively. The cascade control structure provides linearized actuator dynamics for the MPC and enables manual control of the input variables to the OPR.

The robustness towards input disturbances is increased by the estimations in the extended Kalman Filter. This allows the process to continue operation, even in situations that would normally lead to a process shutdown or even an emergency shutdown. Therefore less down-time improves the productivity of the OPR.

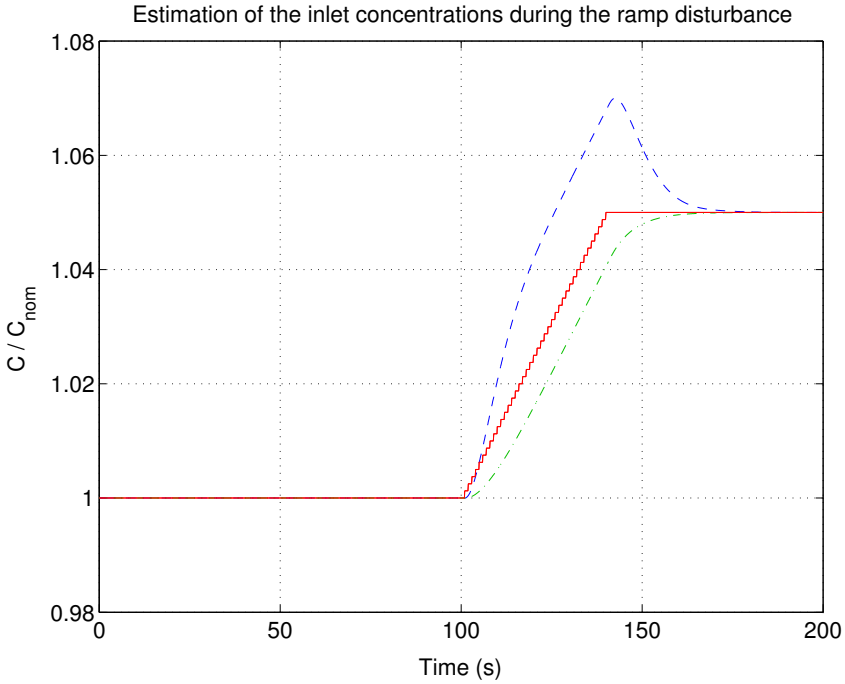

Figure 4.12 Estimation of the inlet concentration for Thiosulfate (dashed) and Hydrogen Peroxide (dash-dot) during ramp disturbance (solid). Each concentration is normalized with its nominal value before the disturbance.

5

The utility system, process and control design

In this chapter, the utility system for the OPR will be presented and controlled. The utility system is a general purpose hydraulic and thermodynamic system that can deliver water with arbitrary temperature and flow rate to control the OPR. In this thesis it has been used as a cooling system and is therefore referred to as either cooling system or utility system.

In Section 5.1, the process design phase is presented. In Section 5.2 the mid-ranging control structure is presented. The control design and tuning is discussed in Section 5.3. The experimental set-up at Alfa Laval AB in Lund is presented in Section 5.4. In Section 5.5 the controller hardware equipment is briefly presented. Disturbances during the experiments are discussed in Section 5.6. The experimental results are shown in Section 5.7 and some concluding remarks on the utility system are summarized in Section 5.8.

5.1 Hydraulic and thermodynamic design

To get the desired flow rate and temperature of the cooling water, given by the optimization in Eq. (4.1), into the cooling plates of the OPR, a utility system has been designed and tested. The hydraulic and thermodynamic design was done by Rolf Christensen at Alfa Laval AB in Lund. Common for all flow configurations below is that an external

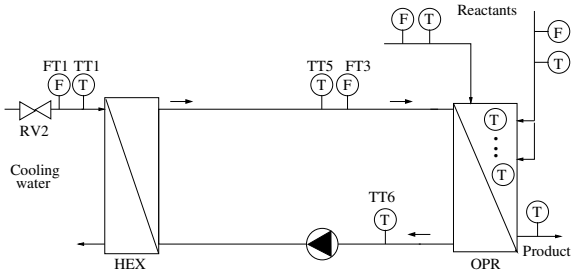

Figure 5.1 Flow configuration 1 with an external heat exchanger to prevent polluted water entering the OPR and cause fouling.

heat exchanger is used. It serves two purposes. First it allows a closed hydraulic system for the water cooling the OPR, since the cooling water, entering from the left in Figure 5.1, may be polluted and may lead to fouling inside the OPR. Now the external heat exchanger can be easily disconnected and removed for cleaning. Secondly, the heat exchanger gives better temperature control of the OPR.

The first naive version is a single flow loop with an external heat exchanger HEX, where the cooling inlet temperature $TT5$ is controlled by varying the flow rate $FT1$ on the left side of HEX, see Figure 5.1. There are several disadvantages with this design. First, there is rarely a need to cool the entire water flow due to the limited heat generation in the plate reactor compared to emergency needs, for which the heat exchanger is designed. Secondly, there is some, although not large, thermal inertia inside the heat exchanger making the control slow.

The second alternative is therefore a system with variable recycle of the cooling flow from the outlet of the OPR, directly to port B of the control valve RV1, see Figure 5.2. With a three-way control valve, the appropriate cooling temperature $TT5$ can be reached by mixing water with the two temperatures $TT6$ and $TT3$. One part of the flow would go to the control valve RV1 directly, the other part would pass through the heat exchanger HEX and then to the control valve. The response of the system is faster than for the first alternative and control of the temperature easier. The flow through the heat exchanger would be variable, depending on the valve position RV1. The flow $FT2$ would

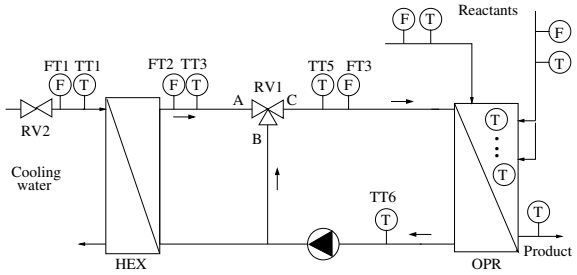

Figure 5.2 Flow configuration 2 with a three-way control valve

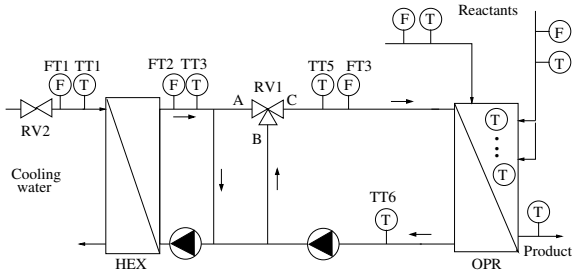

Figure 5.3 Flow configuration of the cooling system with recycle loops around the heat exchanger (HEX) and the OPR. Note that the control signals v_1 and v_2 corresponds to the positions of control valves RV1 and RV2. The output signal u_2 in Figure 4.2 refers to the cooling inlet temperature TT5.

also always be smaller than the flow $FT3$ through the sandwich plates and affecting $TT3$ when it varies. This would lead to the system being sensitive to flow variations in $FT1$.

A third alternative is seen in Figure 5.3, where another recycle loop is around the heat exchanger HEX. Two pumps are needed compared to one pump in the two first alternatives, but with this set-up, the flow rates through the heat exchanger and the sandwich plates are almost constant, regardless of valve position. In the third alternative, the possible flow rate through the heat exchanger is more flexible, so the heat exchanger can be used more adequately. With a higher flow

rate, the heat exchanger is also less sensitive to disturbances in $FT1$.

This flow configuration is common in for example heating systems for houses and in pasteurization units for food applications, [Petitjean, 1994]. The recycles give a fast and less sensitive system, but one should be careful when introducing recycle in the process, since it can lead to large changes in the process dynamics, [Morud and Skogestad, 1996]

Modeling of the utility system

To better understand how the cooling system works, an energy balance is derived around the control valve RV1.

$$(q_{AC} + q_{BC})c_p\rho TT5 = q_{AC}c_p\rho TT3 + q_{BC}c_p\rho TT6 \quad (5.1)$$

$$TT5 = \frac{q_{AC}}{q_{AC} + q_{BC}}TT3 + \frac{q_{BC}}{q_{AC} + q_{BC}}TT6 \quad (5.2)$$

where q_{AC} is the flow rate through valve port A and q_{BC} through port B, see Figure 5.3. Note that this is a simple mixing process with two flows of different temperatures.

Now define the flow ratio as the amount of flow through the control valve port A divided by the flow through port C, which is the sum of the flows through port A and B.

$$\beta = \frac{q_{AC}}{q_{AC} + q_{BC}} \quad (5.3)$$

β can take values from 0 to 1, where 0 corresponds to port A being fully closed and 1 to port B being closed.

The temperature TT5 that should be controlled is then given by

$$TT5 = (TT3 - TT6)\beta + TT6 \quad (5.4)$$

where β can be seen as the manipulated variable. From Eq. 5.4 we see that the process gain is varying depending on the temperatures in the utility system and that the gain is negative, since $TT6 > TT3$ (if the utility side is cooling the reactor). Remember that we have here

neglected the very fast valve dynamics and the short transport delay from valve to sensor.

Apart from the feedback signal from $TT5$, the controller could use measurements from $TT6$ and $TT3$ in a feed forward term to increase its robustness to varying input variables. So far experiments have shown that feedback alone can deal with variations in $TT6$ and $TT3$ very well, see Figure 5.13.

Before the construction of the experimental unit, a more systematic model of the utility system was derived to learn more about the system, what the limitations were and the dynamics of the system. The thermodynamic and hydraulic equations were derived for each component such as pumps, control valves, adjustment valves and a simple heat exchanger model. The model was implemented in Modelica and simulated in Dymola, see [Modelica Association, 2000] and [Dynasim, 2001]. The utility system model was then connected to the OPR model in order to simulate the combined system. After the experiments had been carried out, the model was verified and re-tuned with the experimental data, in terms of time constants of the valves and the thermal inertia.

5.2 Mid-ranging control structure

The cooling temperature $TT5$ should follow the reference temperature $TT5_{ref}$, given by the MPC optimization, see Section 4.7. The main control signal v_1 of the temperature controller is the desired position of the control valve RV1. The valve opening gives the flow ratio β, i.e. how much of the flow that goes through port A divided by the total flow through port C, see Figure 5.3. The second control signal v_2 is the position of control valve RV2, which indirectly controls the temperature $TT3$. By combining the two control signals in a mid-ranging control structure, see Figure 5.4, the cooling temperature $TT5$ can be controlled, and the extra degree of freedom is used to have the control valve RV1 work around some desired operating point, e.g. 50%, to avoid valve saturation.

The term mid-ranging, see for example [Allison and Isaksson, 1998], refers to a control structure that can be used when the process has two input and one output variable. The control signal v_1 takes care of fast

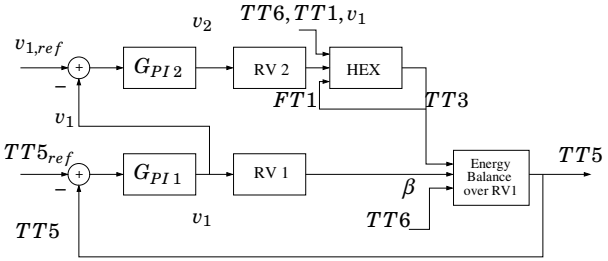

Figure 5.4 Mid-ranging control structure of the utility system. PI-controller G_{PI1} controls the cooling inlet temperature $TT5$ and G_{PI2} acts such that v_1 works around a desirable working point specified by $v_{1,ref}$.

changes, while v_2 acts such that v_1 can operate around a desirable operating point. Due to saturation limits, v_1 should often work in the middle of its operating range, hence the name mid-ranging. In this case, the fast controller v_1 is designed based on the fast dynamics of control valve RV1, while the slower controller v_2 is designed based on the combined dynamics of RV2 and the heat exchanger HEX, which are slower.

There are several advantages with the mid-ranging structure compared to the case when only RV1 is the manipulated input and RV2 has a constant value, giving a constant cooling flow rate $FT1$. First, the operating range of the utility system is largely increased and valve saturation can be avoided. Second, the performance can be increased for large set-point changes. Third, the utility system will be less sensitive to external disturbances. The disadvantage is that v_2 will act as a load disturbance to v_1, which might decrease the transient performance. This can be avoided by introducing a feed forward signal from v_2 to v_1, see [Karlsson *et al.*, 2005].

Another way to see mid-ranging control is that we use two control variables with different frequency content. RV1 gives faster response in $TT5$, but have a small steady-state gain, which gives a small operating range. Whereas RV2 is slower, but with a much greater steady-state gain, giving larger operating range. In Figure 5.5, the Relative Gain Array (RGA) is shown for the utility system. It is normally used to see

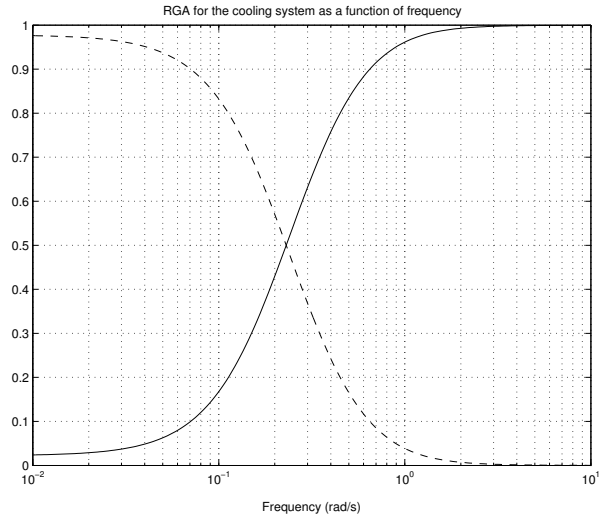

Figure 5.5 Relative Gain Array for the utility system when controlling the cooling temperature $TT5$ with valves RV1 and RV2. The control valve RV1 (solid) dominates for high frequencies, but for low frequencies RV2 (dashed) has greater impact on the cooling temperature.

which input variables that should be used for control in multi-input multi-output systems and how to pair them with output variables. In the figure we see that RV2 (dashed) dominates for low frequencies due to its large steady-state gain. For medium and high frequencies, which is the region where the closed loop bandwidth is, RV1 clearly dominates. However, instead of choosing either of these valves for control, the mid-ranging control technique coordinates *both* control valves to improve performance.

5.3 Control design and tuning

Control design

The nonlinear model of the utility system described in Section 5.1 and

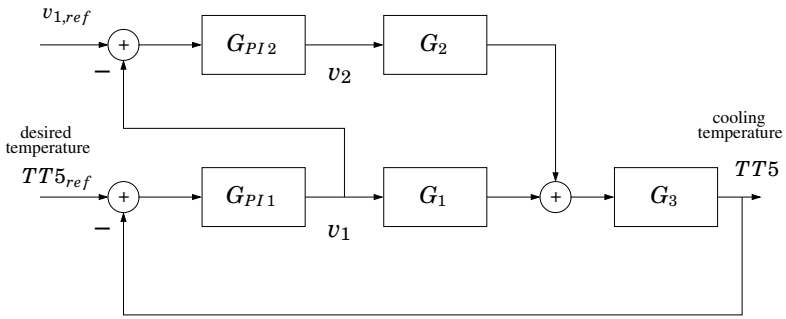

Figure 5.6 Mid-ranging control structure with transfer functions G_1 and G_2, derived from linearization of the utility model after experimental verification.

seen in Figure 5.4 is linearized and the corresponding block diagram can be seen in Figure 5.6. The cooling inlet temperature TT5 can for example be expressed as

$$TT5 = G_3 \begin{bmatrix} G_1 & G_2 \end{bmatrix} \begin{bmatrix} v_1 & v_2 \end{bmatrix}^T \tag{5.5}$$

where v_1 and v_2 are the two valve positions. G_1 represents the valve dynamics of RV1, G_2 represents the valve and heat exchanger dynamics and G_3 represents the mixing of the two water flows and the transport delay between valve and temperature sensor. Bode diagrams of the transfer functions from v_1 and v_2 to the cooling temperature $TT5$ can be seen in Figure 5.7. Note the distinctive differences in cross-over frequency and steady-state gain, which makes the system suitable for mid-ranging. The controllers G_{PI1} and G_{PI2} in Figure 5.6 are two PI-controllers with nonlinear gain to compensate for the nonlinear valve characteristics, see Figure 5.8.

First the nominal controller G_{PI1} is tuned to give good set-point tracking and load disturbance rejection performance. The controlled variable is the temperature of the cooling water $TT5$. We want $TT5$ to track a given reference value $TT5_{ref}$. It is controlled by manipulating the position of the control valve RV1. Mid-ranging control is then achieved by tuning G_{PI2}, so that v_1 can work around its reference value

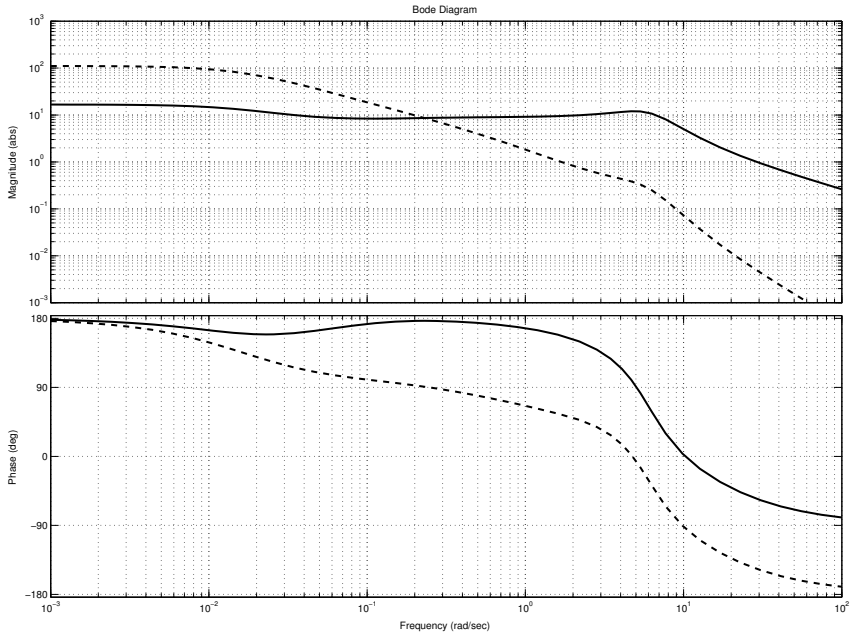

Figure 5.7 Bode diagrams of the transfer functions from v_1 (solid) and v_2 (dashed) to the cooling temperature $TT5$.

$v_{1,ref}$. G_{PI2} should be tuned to a slower response than G_{PI1} not to excite cross-coupling effects. These effects can also be reduced by adding a feed forward term from v_2 to v_1, see for instance [Karlsson *et al.*, 2005].

Control tuning

We start with a basic feedback PI-controller, see [Åström and Hägglund, 1995] and the control law

$$v_{ref} = K(TT5_{ref} - TT5) + \frac{K}{T_i}\int_0^t (TT5_{ref} - TT5)d\tau \tag{5.6}$$

The controller sends a valve position reference, v_{ref}, to the control valve, which uses an internal P-controller with a constant offset to reduce the steady-state error. However the valve characteristic, that is,

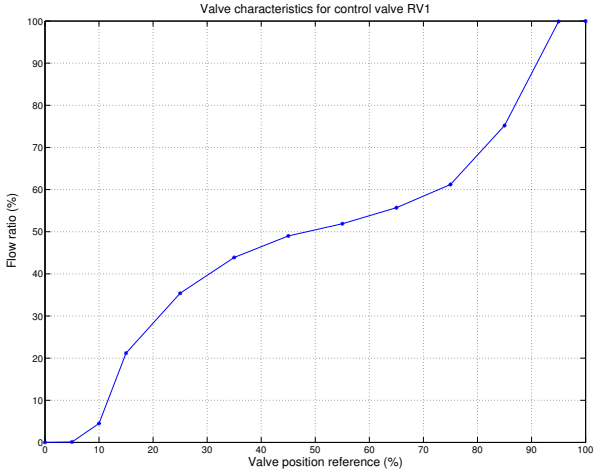

Figure 5.8 Valve characteristics, flow ratio as function of valve position

the flow ratio as a function of valve position $\beta = f(v)$, is nonlinear and should be compensated for. For constant pump speeds, the nonlinear relation has been experimentally measured, see Figure 5.8.

The valve process gain at the end positions is up to 10 times larger than the gain at the middle of the valve range. A controller with constant gain would need to be tuned extremely conservative to be robust towards these large gain variations. This nonlinear valve gain is a good reason to use mid-ranging control, since it allows the control valve RV1 to operate around its linear range at 50%. In addition, we can also use the estimated valve characteristics from Figure 5.8 and include its inverse in the controller. The desired flow ratio β_{ref} is sent through the inverse of the valve characteristics to get the desired valve position. The inverse of the characteristics will therefore serve as a basic form of gain scheduling. The function from β to TT5 is then linearized, since we cancel the nonlinear effects from the valve with the known inverse. The control law becomes

$$\beta_{ref} = K(TT5_{ref} - TT5) + \frac{K}{T_i}\int_0^t (TT5_{ref} - TT5)d\tau \quad (5.7)$$

$$v_{ref} = f^{-1}(v) \quad (5.8)$$

The PI-controllers can for instance be tuned using the λ-method, described in [Åström and Hägglund, 1995].

5.4 Experiments on the utility system

Objectives with the experiments

There were several objectives with the experiments: First, to verify the hydraulic and thermodynamic design of the utility system;Second, to analyze the coupling between the plate reactor and the utility system including the sensitivity to disturbances; Third, to design a control system for the utility system.

The experimental set-up

An experimental set-up was constructed at the test lab of Alfa Laval AB in Lund. Rolf Christensen at Alfa Laval AB performed the hydraulic and thermodynamic design of the test unit, see Figure 5.9. Anders Håkansson at Adesign made the mechanical design. The test unit, see Figure 5.10, was assembled at Alfa Laval AB in Lund by local personnel. The electrical system was designed and installed by Pakon AB.

The OPR was assembled with one reactor plate and two cooling plates, one on each side of the reactor plate. For the tests of the cooling system, it was sufficient to have a similar heat generation inside the OPR as from exothermic reactions. For simplification, instead of using chemical reactants giving exothermic reactions, water was used as reactant A and super-heated steam was used as reactant B. The steam is injected along the side of the OPR.

Methodology

The experiments were carried out in the test lab of Alfa Laval AB in Lund, Sweden. The test rig is extensively instrumented in order to monitor all important variables and properties of the system. The experiments were carried out in a specific order to ensure that all components had full functionality before the main tests were done. Every component was checked individually and every sub system was tested

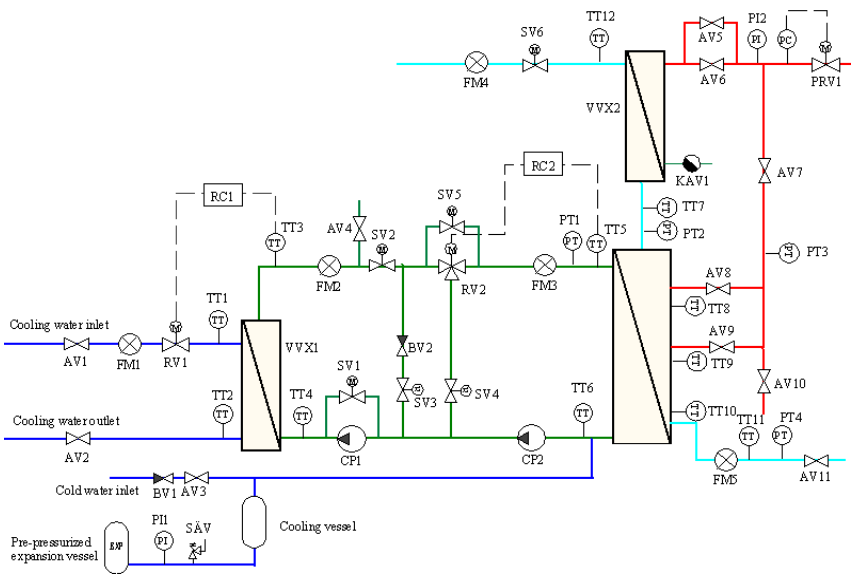

Figure 5.9 Experimental flow scheme

before it was used in the complete process. All experiments have been carefully planned, in order to have full reproducibility of the experimental results. However, the manual-operated steam system prevented exact and full reproducibility for some experiments. The steam injections have therefore been used mainly to get a desired heat load inside the reactor to test the utility system and its control system. A full survey of existing disturbances was carried out, if possible to eliminate them and if not to be aware of them and take them into consideration during the experiments, see Section 5.11.

5.5 Control system hardware

To have a large flexibility in performing the experiments, the test unit has two parallel independent control systems. With a simple switch the user can choose which control system he wants to use for an exper-

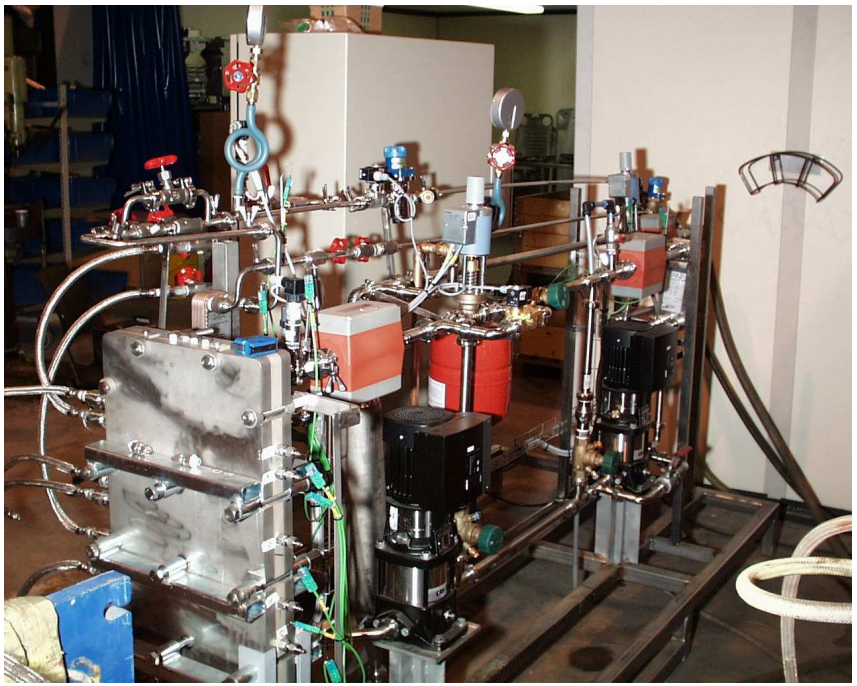

Figure 5.10 The experimental setup at Alfa Laval laboratory in Lund. The OPR is seen to the left and the utility system to the right. Note the injection pipes on the left side of the OPR and the thermocouples along the right hand side of the OPR.

iment. The signals from each sensor are duplicated and sent to each of the control systems. The control systems then computes the appropriate actions, but only the output signals from the selected control system are sent to the control valves and the pumps. The control systems will also have a process supervision task, which is connected to an automatic safety system.

The first control system is made by components from National Instruments and centered on their software package LabVIEW, [National Instruments, 2005]. The software enables easy configuration with their hardware components, such as data acquisition cards and analog out-

put cards. The actual control algorithms and all process monitoring are done entirely in the LabVIEW software, thus giving high flexibility for testing new features without having to change any hardware.

The second control system is centered around an ECA controller from ABB with two PID control loops available, [ABB, 2000]. The system is hardware-oriented and functions and features are done with separate hardware components instead of in software. The system is more similar to commercial systems than LabVIEW.

All measurements are sent to a TopMessage logger from Delphin. The logger samples the 30 measurements with a sampling frequency of around 5 Hz. The logger sends the data to a PC through an OPC-server to the data acquisition program EasyView5 [Intab, 2005] from Intab AB.

5.6 Disturbances and process variations

Before the experiments were started, a rough analysis of potential disturbances was made. The plate reactor system has several input signals, all vulnerable to disturbances from the surroundings. The test rig was placed in the test lab of Alfa Laval in Lund, where many other experiments were carried out at the same time. All experiments take water from the central water system, which transfers possible disturbances from one experiment to another.

When a large pump is started anywhere in the lab, the pressure in the water system decreases for a very short moment. The process flow rate to the plate reactor, $FT4$ and the flow rate to the heat exchanger, $FT1$ are therefore also decreased for a short period of time. When the pump stops, the pattern is repeated but in opposite direction. When the pump actions are periodic, we get periodic disturbances in these signals, see Figure 5.11.

Another disturbance in the flow rate $FT4$ is when high-pressured steam is injected into the reactor. When steam is injected, the pressure inside the reactor increases and the flow rate $FT4$ decreases. The steam injection causes the pressure before and after the reactor to vary rapidly, thus causing very fast disturbances in the flow rates to and from the reactor $FT4$ and $FT5$, which can be seen in Figure 5.11 from time 13.28. The variation in $FT1$ does not cause any significant variation in $TT3$, due to the low pass filter effect of the heat exchanger VVX1. The effect from the $FT4$-variations on the reactor temperature is larger, since the process flow is pre-heated in the small heat exchanger VVX2 with a constant steam flow and if the process flow is varying the process inlet temperature will also vary. In a real production unit there would not be any of these variations, at least not in the process flow since there would be individual pumps for each reactant. The disturbances are however interesting, since they give us information about the dynamics and sensitivities of the system that we otherwise would not get.

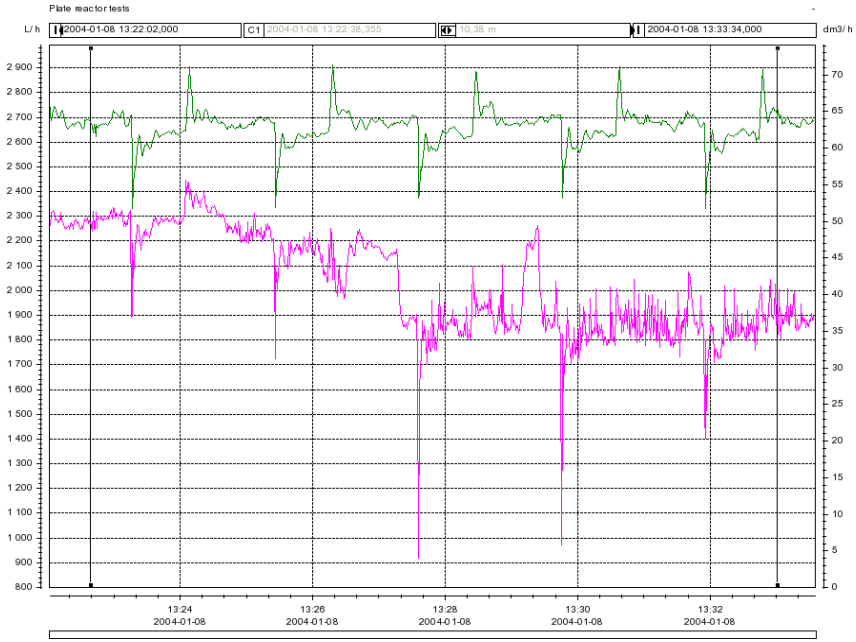

Figure 5.11 Measurement of process disturbances in the two flows $FT1$ and $FT4$, during utility system experiments. The disturbances enter the main water system roughly every two minutes.

The chain of measurement equipment "thermocouples - transmitters - resistors" were calibrated at five different temperatures with a

Pt-100 sensor as reference. The differences between individual measurements were large, at most 3°C. However, the largest cause for the differences was not the thermocouples, but the transmitters and the resistors. Some thermocouples have during the experiments given inaccurate measurements from time to time and likely causes can for example be steam bubbles inside the reactor or glitches. Especially the thermocouples inside the reactor have given noisy data during steam injection.

5.7 Experimental results

In Figure 5.12 we can see step responses in $TT5$ for the controller in Eq. (5.8) without and then with the nonlinear gain compensation for the nonlinear valve characteristics. For notations, see Figure 5.3. The PI-controller was auto-tuned with relay experiments around the 40 % operating point with $K = 3.0$ and $T_i = 1.0$ s. The step in $TT5_{ref}$ is from 25.4°C to 29.4°C. When the control valve is near its end position, RV1 = 5 %, the process gain from valve position to flow ratio is considerably larger than in the middle of the valve range, which was seen in Figure 5.8. Due to the increased process gain at this operating point the closed loop system becomes unstable, as seen around $t = 20$ s in Figure 5.12. The nonlinear gain compensation of the valve characteristics is enabled at $t = 35$ s and the system returns to the new set-point. The step response is repeated at time $t = 75$ s using the nonlinear gain compensation from start and the step response of the closed loop system is then stable and well-damped.

The next experiment is to keep the cooling inlet temperature TT5 constant despite load disturbances inside the reactor. The flow rate of the injected steam is suddenly decreased, thus reducing the heat release inside the OPR by 50%. This causes the cooling water to be less heated and the cooling outlet temperature TT6 decreases. Due to the recycle loops, the cooling inlet temperature TT5 is quickly effected, unless necessary control actions are made. In this experiment, the mid-ranging control was disabled and only the PI-controller for RV1 was active. In Figure 5.13 it can be seen that the controller manages to keep the cooling temperature TT5 almost constant, despite the large change in heat release and cooling outlet temperature TT6.

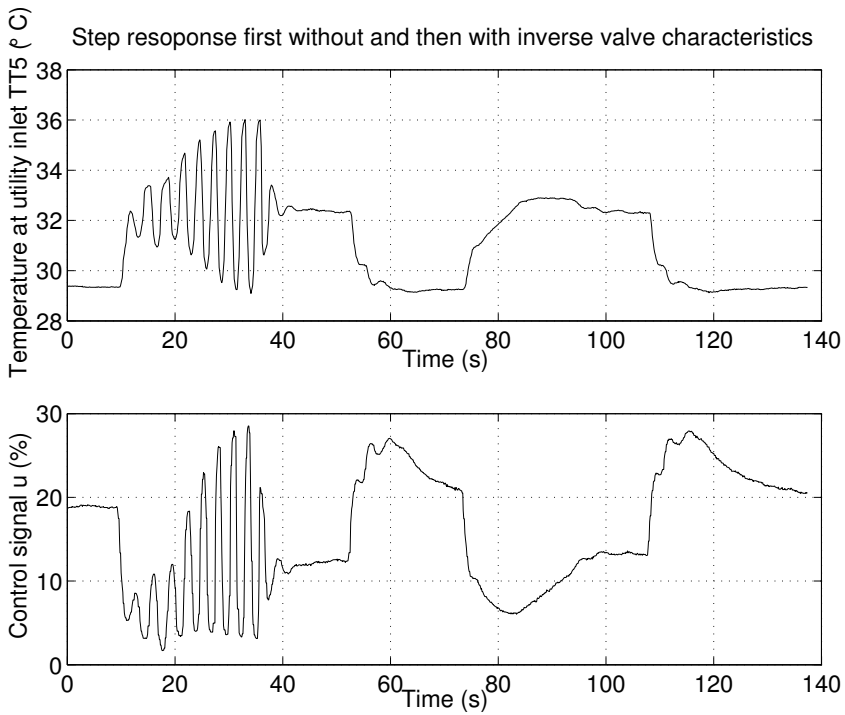

Figure 5.12 Step response first without and then with the inverse valve characteristics as nonlinear gain compensation.

The mid-ranging control structure is also tested in a series of experiments, see Figure 5.14. A step sequence in temperature reference is made first without mid-ranging, where v_2 (solid) is constant, leading to a constant cooling flow rate $FT1$. The step sequence is then repeated using mid-ranging, which is tuned rather aggressively to clearly illustrate the mid-ranging effect. The control parameters for v_1, the first PI-controller, are the same for both experiments. After the first step in the reference signal, the control valve v_1 (dashed) position goes down from 50% to 20% open, which can severely limit the operating range of the cooling system. The mid-ranging is enabled at $t = 240$ s. With the mid-ranging, the v_1 returns to 50% after about 30 seconds. There is

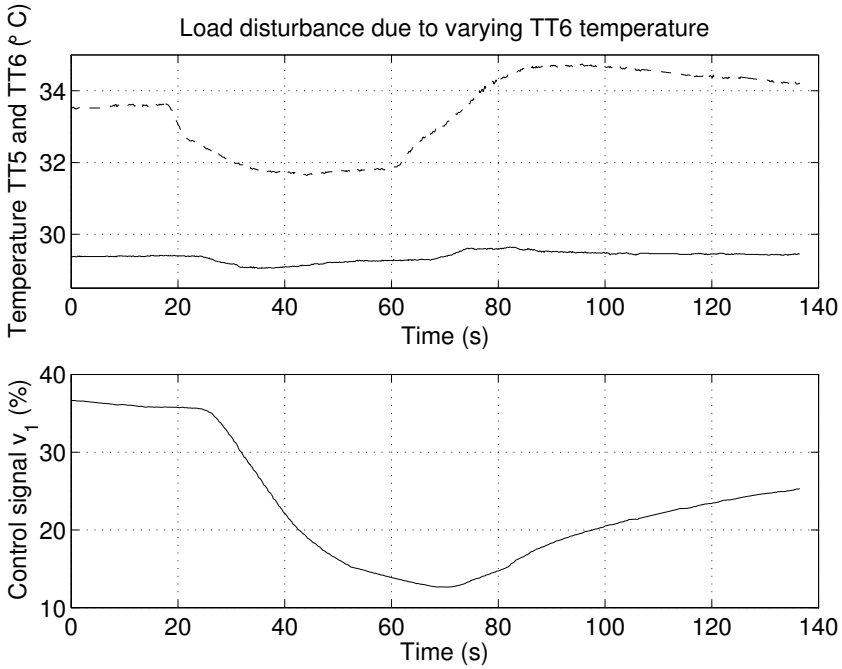

Figure 5.13 Load disturbance experiments. The heat release inside the plate reactor is suddenly decreased, which directly affects the outlet cooling temperature TT6 (dashed). The controlled variable TT5 (solid), the cooling inlet temperature, remains almost constant.

however a small increase in the overshoot of the step response, due to the mid-ranging control and the cross-couplings in the cooling system. These effects can be reduced by re-tuning the mid-ranging controller G_{PI2} for a more reasonable response.

5.8 Summary of the utility system and its controller

The utility system is a multi-purpose heating/cooling system and should be able to serve any other process as well. However in this project, the

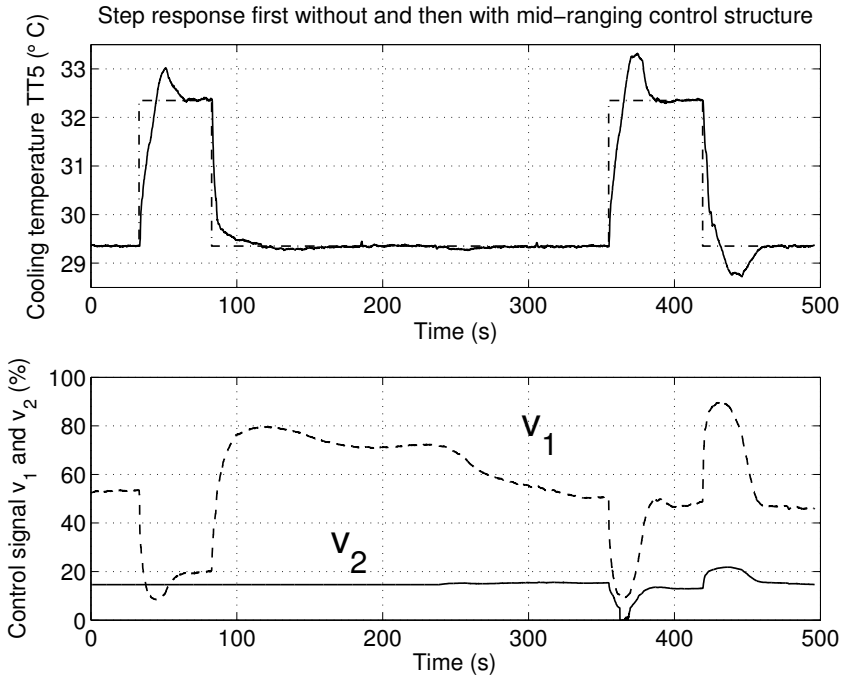

Figure 5.14 Step response experiments. Top plot: cooling temperature (solid) and its reference (dash-dot). Lower plot: the two control signals v_1 and v_2. Note that during the first step mid-ranging is disabled and for the second step, the mid-ranging controller is tuned rather aggressively to clearly illustrate its effect on v_1.

utility system is designed to allow fast and flexible temperature control of the OPR.

To reduce fouling inside the cooling plates of the OPR, a closed flow circuit of water is used and an extra heat exchanger transfers heat from the cooling water to some cooling reservoir, for example a river. Recycle loops are introduced to improve the speed of the response of the system and to reduce the sensitivity to external disturbances.

A mid-ranging controller is designed, which uses two control valves to control the cooling temperature and reduces the risk of valve sat-

uration. The mid-ranging control technique improves drastically the flexibility of the utility system and increases its operating range with existing equipment.

The utility system and its control system are verified in a series of experiments. The controller offers very good set-point tracking and disturbance rejection.

6

Summary

The Open Plate Reactor has been presented and its new features in terms of flow channel inserts, internal sensors, multiple injection points and cooling plates have been discussed. The open configuration enables very precise temperature control of the reactor. Our findings show the OPR to be a very flexible tool for producing high-quality chemicals effectively.

A nonlinear state-space model of the OPR has been derived from first principle. The model is used for analysis of the input variables to find suitable control variables. It has been shown that by manipulating the reactant distribution and the cooling temperature, the temperature maximum after each injection point can be arbitrarily controlled. To our knowledge, this has not been thoroughly investigated previously. To enable the implementation of this control strategy, the process design utilizes control valves to allow accurate flow control of the reactants. This is one example of the fruitful interactions between process design and control design.

In the thesis three important control aspects have been discussed; temperature constraints, conversion optimization and state estimation. Model predictive control combines the explicit handling of constraints with optimization of the conversion. This allows for operation closer to the constraints, thus increasing productivity and conversion. Secondly, for more complex reaction schemes, the model-based optimization solves the non-trivial problem of finding suitable reactor temperatures that maximize the conversion.

An extended Kalman filter was applied for estimation of unmea-

sured concentrations. Disturbance estimation was used to reduce the impact from variations in the feed concentrations. There are model errors introduced for example by linearizing the process model as well as from unmodeled dynamics. More research is therefore needed on how to consider model errors in the control design, see for example [Findeisen *et al.*, 2003] for nonlinear MPC, allowing use of nonlinear process models, and [Wang and Rawlings, 2004a; Wang and Rawlings, 2004b] for robust MPC. Another approach may be to use adaptive methods, such as extremum seeking control to estimate uncertain reaction kinetics, [Hudon *et al.*, 2005].

A utility system has been experimentally tested with a mid-ranging temperature controller. It can deliver cooling or heating water to the OPR with a desired temperature that is given by the MPC optimization. The mid-ranging structure increases largely the operating range of the hydraulic equipment and decreases the sensitivity to the valve nonlinearities. It enables the control valve to operate in a favorable region.

Our investigation utilized only a portion of the possible degrees of freedom allowed by the OPR and the control variables proposed in this thesis can thus be augmented to further increase control flexibility. For example, feed inlet temperatures can be manipulated for start-up control and control of the feed concentrations of the reactants may be used, when possible, to improve productivity online. To allow more accurate control, better online measurement sensors should be developed, especially concentration sensors. Other control properties left to explore are different cooling flows for different parts of the reactor and use of more injection points.

A

Bibliography

ABB (2000): *ECA-600 Processregulatorer*. www.abb.se.

Åkesson, J. (2003): "Operator interaction and optimization in control systems." Licentiate thesis ISRN LUTFD2/TFRT--3234--SE. Department of Automatic Control, Lund Institute of Technology, Sweden.

Åkesson, J. and P. Hagander (2003): "Integral action—a disturbance observer approach." In *Proceedings of European Control Conference*.

Allison, B. J. and A. J. Isaksson (1998): "Design and performance of mid-ranging controllers." *Journal of Process Control*, **8**, pp. 469–474.

Andersson, R., B. Andersson, F. Chopard, and T. Norén (2004a): "Development of a multi-scale simulation method for design of novel multiphase reactors." *Chemical Engineering Science*, **59**, pp. 4911–4917.

Andersson, R., M. Bouaifi, and B. Andersson (2004b): "Computational fluid dynamics simulation of the dispersed phase size distribution in a multifunctional channel reactor." *Chemical Engineering Research and Design Journal*, **submitted**.

Åström, K. J. and T. Hägglund (1995): *PID Controllers: Theory, Design, and Tuning*. Instrument Society of America, Research Triangle Park, North Carolina.

Åström, K. J. and B. Wittenmark (1997): *Computer-Controlled Systems*. Prentice Hall.

Bouaifi, M. and B. Andersson (2004): "Hydrodynamics and gas-liquid mass transfer in a new multifunctional channel reactor." *Chemical Engineering Research and Design Journal*, **submitted**.

Bouaifi, M., M. Mortensen, R. Andersson, W. Orciuch, B. Andersson, F. Chopard, and T. Norén (2004): "Experimental and numerical cfd investigations of a jet mixing in a multifunctional channel reactor : Passive and reactive systems." *Chemical Engineering Research and Design Journal*, **82**, pp. 274–283.

Chopard, F. (2001): "Patent: FR 0105578, Improved device for exchange and/or reaction between fluids, PCT WO 02/085511."

Chopard, F. (2002): "Patent: SE 0203395.9, Flow directing insert for a reactor chamber and a reactor, PCT WO 20/04045761."

Christofides, P. (2001): *Nonlinear and robust control of PDE systems. Systems and control: Foundations and applications.* Birkhäuser.

Dochain, D. (2003): "State and parameter estimation in chemical and biochemical processes: a tutorial." *Journal of Process Control*, **13**, pp. 801–818.

Dynasim (2001): *Dymola, Dynamic Modeling Laboratory - User's Manual*. Dynasim AB.

Findeisen, R., L. Imsland, F. Allgöwer, and B. Foss (2003): "State and output feedback nonlinear model predictive control: An overview." *European Journal of Control*, **9**, pp. 190–206.

Fogler, S. (1992): *Elements of chemical reaction engineering*. Prentice Hall.

Green, A., B. Johnson, and A. John (1999): "Process intensification magnifies profits." *Chemical Engineering*, **106**, p. 66.

Hägglund, T. (2001): "The Blend station - a new ratio control structure." *Control Engineering Practice*, **9**, pp. 1215–1220.

Haugwitz, S. and P. Hagander (2004a): "Mid-ranging control of the cooling temperature for an Open Plate Reactor." In *Proceedings of the 12th Nordic Process Control Workshop*.

Haugwitz, S. and P. Hagander (2004b): "Temperature control of a utility system for an Open Plate Reactor." In *Proceedings of Reglermöte*.

Haugwitz, S. and P. Hagander (2005): "Process control of an Open Plate Reactor." In *Proceedings of IFAC World Congress*.

Hudon, N., M. Perrier, M. Guay, and D. Dochain (2005): "Adaptive extremum seeking control of a non-isothermal tubular reactor with unknown kinetics." *Computers and Chemical Engineering*, pp. 839–849.

Intab (2005): *Easyview 5.5, Efficient and complete software for graphing data*. www.intab.se.

Karafyllis, I. and P. Daoutidis (2002): "Control of hot spots in plug flow reactors." *Computers & Chemical Engineering*, **26**, pp. 1087–1094.

Karlsson, M., O. Slätteke, B. Wittenmark, and S. Stenström (2005): "Reducing moisture transients in the paper-machine drying section with the mid-ranging control technique." *Nordic Pulp and Paper Research Journal*, **20:2**, pp. 150–156.

Liu, Y. (2005): *Grey-box Identification of Distributed Parameter Systems*. PhD thesis, Royal Institute of Technology (KTH). TRITA-S3-REG-0503.

Logist, F., I. Smets, and J. V. Impe (2005a): "Optimal control of dispersive tubular chemical reactors: Part I." *Proceedings of IFAC World Congress*.

Logist, F., I. Smets, and J. V. Impe (2005b): "Optimal control of dispersive tubular chemical reactors: Part II." *Proceedings of IFAC World Congress*.

Luyben, W. (2001): "Effect of design and kinetic parameters on the control of cooled tubular reactor systems." *Industrial & Engineering Chemistry Research*, **40**, pp. 3623–3633.

Maciejowski, J. M. (2002): *Predictive Control with Constraints*. Pearson Education Limited.

Modelica Association (2000): *Modelica - A Unified Object-Oriented Language for Physical System Modeling*. www.modelica.org.

Morud, J. and S. Skogestad (1996): "Dynamic behaviour of integrated plants." *Journal of Process Control*, **6**, pp. 145–156.

National Instruments (2005): *LabVIEW 7.1, Graphical programming for engineers and scientists*. www.ni.com.

Nilsson, J. and F. Sveider (2000): "Characterising mixing in a hex reactor using a model chemical reaction." http://www.chemeng.lth.se/exjobb/002.pdf.

Pannocchia, G. and J. Rawlings (2003): "Disturbance models for offset-free model predictive control." *AIChE Journal*, **49**, pp. 426–437.

Petitjean, R. (1994): *Total hydronic balancing*. Tour and Andersson.

Phillips, C., G. Lausche, and H. Peerhossaini (1997): "Intensification of batch chemical process by using integrated chemical reactor heat exchangers." *Applied Thermal Engineering*, **17**, pp. 809–824.

Qin, S. and T. Badgwell (2003): "A survey of industrial model predictive control technology." *Control Engineering Practice*, **11**, pp. 733–764.

Ramshaw, C. (1995): "The incentive for process intensification." *In Proceedings 1st Intl. Conf. of Process Intensification for Chem. Ind.*, **18**.

Renou, S., M. Perrier, D. Dochain, and S. Gendron (2003): "Solution of the convection-dispersion-reaction equation by a sequencing method." *Computers and Chemical Engineering*, **27**, pp. 615–629.

Shang, H., J. Forbes, and M. Guay (2002): "Characteristics-based model predictive control of distributed parameter systems." *In Proceedings of the American Control Conference*, pp. 4383–4388.

Shang, H., J. F. Forbes, and M. Guay (2005): "Feedback control of hyperbolic distributed parameter systems." *Chemical Engineering Science*, **60**, pp. 969–980.

Shinskey, F. (1996): *Process Control Systems*. McGraw-Hill.

Smets, I., D. Dochain, and J. V. Impe (2002): "Optimal temperature control of a steady-state exothermic plug-flow reactor." *AIChE Journal*, **48**, pp. 279–286.

Stankiewicz, A. and J. Moulin (2000): "Process intensification: Transforming chemical engineering." *Chemical Engineering Progress*, **96**, pp. 22–34.

Stein, G. (2003): "Respect the unstable." *IEEE Control Systems Magazine*, **23**.

Thomas, P. (1999): *Simulation of Industrial Processes*. Butterworth-Heinemann.

Wang, Y. and J. Rawlings (2004a): "A new robust model predictive control method I: theory and computation." *Journal of Process Control*, **14**, pp. 231–247.

Wang, Y. and J. Rawlings (2004b): "A new robust model predictive control method II: examples." *Journal of Process Control*, **14**, pp. 249–262.

Winkin, J., D. Dochain, and P. Ligarius (2000): "Dynamical analysis of distributed tubular reactors." *Automatica*, **36**, pp. 349–361.

Wouwer, A., P. Saucez, and W. Schiesser (2004): "Simulation of distributed parameter systems using a matlab-based method of lines toolbox: Chemical engineering applications." *Ind. Eng. Chem. Res.*, **43**, pp. 3469–3477.